DOI: 10.1002/chem.200701392

Divalent Carbon(0) Chemistry, Part 2: Protonation and Complexes with Main Group and Transition Metal Lewis Acids

Ralf Tonner and Gernot Frenking*[a]

Abstract: Quantum-chemical calculations with DFT (BP86) and ab initio methods (MP2, SCS-MP2) were carried out for protonated and diprotonated compounds **N-H$^+$** and **N-(H$^+$)$_2$** and for the complexes **N-BH$_3$**, **N-(BH$_3$)$_2$**, **N-CO$_2$**, **N-(CO$_2$)$_2$**, **N-W(CO)$_5$**, **N-Ni(CO)$_3$** and **N-Ni(CO)$_2$** where **N** = C(PH$_3$)$_2$ (**1**), C(PMe$_3$)$_2$ (**2**), C(PPh$_3$)$_2$ (**3**), C(PPh$_3$)(CO) (**4**), C(CO)$_2$ (**5**), C(NHC$_H$)$_2$ (**6**), C(NHC$_{Me}$)$_2$ (**7**) (Me$_2$N)$_2$C=C=C(NMe$_2$)$_2$ (**8**) and NHC (**9**) (NHC$_H$ = N-heterocyclic carbene, NHC$_{Me}$ = *N*-substituted N-heterocyclic carbene). Compounds **1**–**4** and **6**–**9** are very strong electron donors, and this is manifested in calculated protonation energies that reach values of up to 300 kcal mol^{-1} for **7** and in very high bond strengths of the donor–acceptor complexes. The electronic structure of the compounds was analyzed with charge- and energy-partitioning methods. The calculations show that the experimentally known compounds **2**–**5** and **8** chemically behave like molecules L$_2$C which have two L→C donor–acceptor bonds and a carbon atom with two electron lone pairs. The behavior is not directly obvious when the linear structures of carbon suboxide and tetraaminoallenes are considered. They only come to the fore on reaction with strong electron-pair acceptors. The calculations predict that single and double protonation of **5** and **8** take place at the central carbon atom, where the negative charge increases upon subsequent protonation. The hitherto experimentally unknown carbodicarbenes **6** and **7** are predicted to be even stronger Lewis bases than the carbodiphosphoranes **1**–**3**.

Keywords: bonding analysis · carbon · density functional calculations · donor–acceptor systems · protonation

Introduction

In the preceding paper[1] we presented a detailed bonding analysis of the molecules C(PH$_3$)$_2$ (**1**), C(PMe$_3$)$_2$ (**2**), C(PPh$_3$)$_2$ (**3**), C(PPh$_3$)(CO) (**4**), C(CO)$_2$ (**5**), C(NHC$_H$)$_2$ (**6**), C(NHC$_{Me}$)$_2$ (**7**). (Me$_2$N)$_2$C=C=C(NMe$_2$)$_2$ (**8**), and imidazolin-2-ylidene (**9**) by charge- and energy-partitioning methods. We suggested that the bonding situation in **1**–**4**, **6**, and **7**, which have a bent L$_2$C structures, can be explained in terms of donor–acceptor interactions between a bare carbon atom in the singlet (^{1}D) state serving as a Lewis acid which has two lone-pair orbitals and two monodentate Lewis bases (L→C←L). The divalent carbon(0) character of these compounds is revealed by the shape of the frontier orbitals. Compounds **5** and **8**, which have a linear C=C=C moiety, are better described in terms of two double bonds, but the very shallow bending potential indicates that the molecules may show chemical behavior in which the central carbon atom employs two lone-pairs of electrons for chemical bonding. Previous experimental observations whose relevance was apparently overlooked[2] support the idea that compounds like **8** have "hidden" divalent carbon(0) character. The tetraaminoallene (TAA) **8** reacts with the weak Lewis bases CO$_2$ and CS$_2$ to give complexes [(NMe$_2$)$_2$C]$_2$C–CX$_2$ (X = O, S; Scheme 1) in which the central carbon atom of **8** binds to CX$_2$ by a donor–acceptor bond.[3] Another experimental result which points toward the "hidden" double-lone-pair character of TAAs is the finding that upon protonation the compounds may bind two protons at the central carbon atom rather than at nitrogen, for example, to yield

[a] Dipl.-Chem. R. Tonner, Prof. Dr. G. Frenking
Fachbereich Chemie
Philipps-Universität Marburg
Hans-Meerwein-Strasse, 35032 Marburg (Germany)
E-mail: frenking@chemie.uni-marburg.de

Supporting information for this article is available on the WWW under http://www.chemeurj.org/ or from the author.

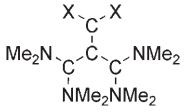

Scheme 1. Complexes of tetraaminoallenes [(NMe$_2$)$_2$C]$_2$C–CX$_2$ (X = O, S) which have been synthesized.[3] Experimental data are not given.

the crystallographically characterized dication $[\{(NHR)_2C\}_2CH_2]^{2+}$ (R = *tert*-butyl).[4] The experimental observations and our theoretical investigations of divalent carbon(0) compounds[1,5] indicate that the donor–acceptor chemistry of **1–8** may lead to surprising new discoveries which should be studied with experimental and theoretical methods.

To see whether the unusual bonding situation in **1–8**, which is revealed by the bonding analysis,[1] has any relevance to their chemical behavior, we calculated complexes in which the divalent carbon(0) compounds serve as Lewis bases. Here we report on quantum chemical calculations using DFT (BP86) and ab initio methods (MP2, SCS-MP2) of the first and second protonation energies of **1–9**. We also calculated donor–acceptor complexes of **1–9** with the Lewis acids BH_3, CO_2, $W(CO)_5$, $Ni(CO)_3$, and $Ni(CO)_2$. The complexes with N-heterocyclic carbene (NHC) **9** were analyzed to investigate the differences between a divalent carbon(II) and a divalent carbon(0) compound in the donor–acceptor complexes. The electronic structure of the molecules was analyzed with charge-and energy-decomposition methods, which are described in the preceding paper.[1]

Methods

Since the theoretical methods which were employed for this work are the same as in the preceding paper,[1] we give only a short summary of the computational part. The geometries of the molecules were optimized at the BP86[6]/SVP[7] level of theory. Energies were calculated with BP86, MP2 and spin-component-scaled (SCS) MP2[8] in conjunction with TZVPP basis sets at BP86/SVP optimized geometries. The above calculations were carried out with the programs Gaussian 03[9] and TurboMole5.[10] All-electron basis sets were used for the atoms except for tungsten, for which a small-core quasi-relativistic ECP was applied.[11] The charge analyses were carried out by using the NBO[12] and AIM[13] partitioning methods. The energy decomposition analysis (EDA)[14] of the donor–acceptor bonds was performed with the program ADF2006.01.[15] For these calculations we optimized the geometries at the BP86/TZ2P level.[16] Scalar relativistic effects were considered by the zeroth-order regular approximation (ZORA) in the ADF calculations.[17] Cartesian coordinates and total energies of all compounds discussed in the text are available as Supporting Information.

Results and Discussion

Main group complexes with ligands 1–9: Divalent carbon(0) compounds have two electron lone pairs which are capable of binding two monodentate Lewis acids, and thus they should be extremely strong Lewis bases. The experimentally observed chemical reactivity indicates that CDPs are indeed strong electron donors.[18–24] To quantify the donor strength of **1–9** we calculated the geometries and the bonding energies of complexes with one and two Lewis acids H^+, BH_3, and CO_2. The most important geometrical variables of L_2C–A and L_2C–A_2 (A = H^+, BH_3 and CO_2) are given in Table 1.

Table 1. Calculated geometrical parameters (bond lengths [Å] and angles [°]) of Lewis acid complexes **1-A** to **9-A** with **A** = H^+, BH_3, CO_2 at BP86/SVP. Experimental values from X-ray analyses are given in italics.

	N-H$^+$			**N-BH$_3$**			**N-CO$_2$**		
N	*d*(C–A)	*d*(C–L)	∢(L-C-L)	*d*(C–A)	*d*(C–L)	∢(L-C-L)	*d*(C–A)	*d*(C–L)	∢(L-C-L)
1	1.102	1.720	126.4	1.685	1.692	124.7	1.498	1.700/ 1.758	133.8
2	1.102	1.730	131.4	1.688	1.696	131.0	1.539	1.730	135.8
3	1.100	1.735 *1.722(4)*[b]	132.4 *131.9(2)*	1.689	1.711	128.2	1.512	1.731/ 1.769	137.0
4	1.103	1.788/ 1.337[d]	123.3	1.713	1.736/ 1.324[d]	121.0		–[e]	
5	1.112	1.370	122.9	1.812	1.331	130.6		–[e]	
6	1.097	1.408	125.6	1.640	1.397	121.1		–[f]	
7	1.099	1.418 *1.413(4)*[g]	126.1 *123.5(3)*	1.665	1.413/ 1.418	117.8	1.588	1.419	120.3
8	1.099	1.422 *1.375(4)*[h]	129.1 *127.1(3)*	1.654	1.417/ 1.426	117.9	1.609	1.417	122.7
9	1.096	1.345 *1.323(4)*[k] *1.333(4)*	106.9 *108.4(2)*	1.587	1.364	103.3	1.556	1.345	106.4

	N-(H$^+$)$_2$			**N-(BH$_3$)$_2$**			**N-(CO$_2$)$_2$**		
N	*d*(C–A)	*d*(C–L)	∢(L-C-L)	*d*(C–A)	*d*(C–L)	∢(L-C-L)	*d*(C–A)	*d*(C–L)	∢(L-C-L)
1	1.116	1.855	122.3	1.698	1.753	120.1	1.589/ 1.593	1.796/ 1.806	127.9
2	1.113	1.861 *1.80(1)*[a] *1.812(9)*	126.5 *121.6(6)*	1.706	1.788	117.6	1.600	1.862	125.4
3	1.110	1.869 *1.816(4)*[c] *1.822(4)*	131.0 *123.4(2)*	1.730	1.810	119.2	1.564/ 1.657	1.870/ 1.899	123.6
4	1.114	2.022/ 1.407[d]	115.8	1.805/ 1.763[d]	1.793/ 1.356[d]	117.0		–[e]	
5	1.136	1.476	115.9	1.917	1.349	127.8		–[e]	
6	1.112	1.508	117.2	1.687/ 1.717	1.468/ 1.474	114.0		–[e]	
7	1.111	1.508	118.3	1.732	1.471	112.2		–[e]	
8	1.109	1.527 *1.511*[i] *1.522*	121.3 *112.5*	1.769	1.468	114.9		–[e]	
9	1.124	1.450	101.1		–[j]			–[e]	

[a] Ref. [29]. [b] Ref. [27]. [c] Ref. [30]. [d] C–PPh_3 bond length/C–CO bond length. [e] Dissociation occurs during optimization. [f] CO_2 deprotonates both NHCs. [g] Ref. [31]. [h] Ref. [32b]. [i] Ref. [32b]. [j] One BH_3 molecule dissociates and forms a B_2H_6 species with η^1-coordination towards the NHC. [k] Ref. [28].

Figure 1 displays the geometries of the complexes with BH_3 and CO_2, which were found as equilibrium structures on the potential-energy surfaces. The geometry optimizations of $L_2C–(CO_2)_2$ did not give minima for tetracoordinate carbon complexes except for the CDPs, which shows that the donor strength of the second electron lone pair is not high enough to bind two weak Lewis acids like CO_2. The full set of geometries is available in Table S1 in the Supporting Information.

Figure 1 also gives experimental values of bond lengths and angles, which are available for **3-BH$_3$**,[24] **3-CO$_2$**,[21] and for substituted derivatives of **9-BH$_3$**[25] and **9-CO$_2$**.[26] Experimental values have also been reported for the protonated compounds **3-H$^+$**,[27] **9-H$^+$**[28] and for the diprotonated species **2-(H$^+$)$_2$**[29] and **3-(H$^+$)$_2$**,[30] as well as for substituted analogues of **7-H$^+$**,[31] **8-H$^+$**[32] and **8-(H$^+$)$_2$**.[32b] The relevant data are given in Table 1. The agreement between theory and experiment is quite good. The experimentally observed

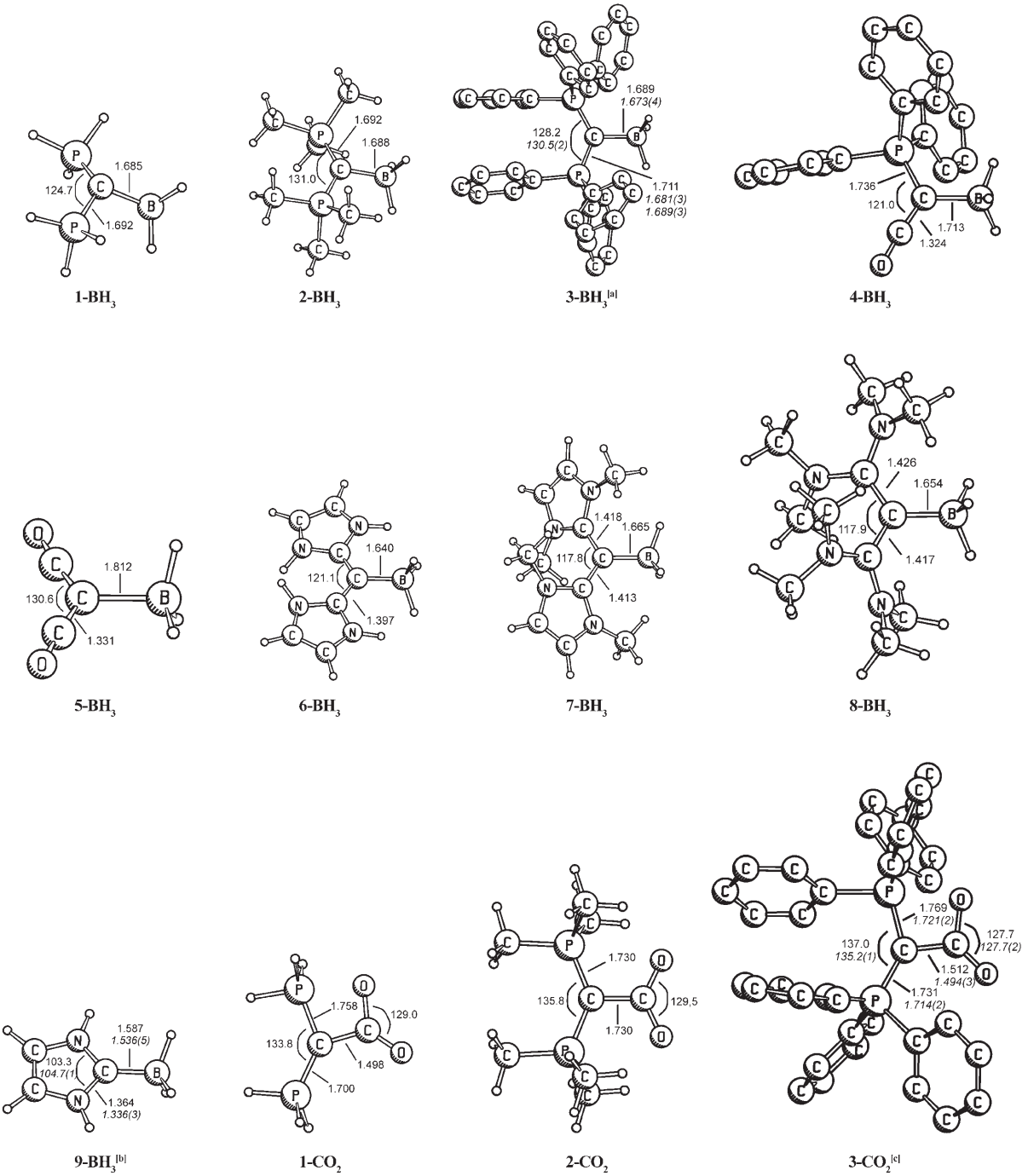

Figure 1. Optimized geometries (bond lengths [Å] and angles [°]) at the BP86/SVP level of **N-BH$_3$**, **N-CO$_2$**, **N-(BH$_3$)$_2$**, and **N-(CO$_2$)$_2$** (**N**=**1**–**9**) which were found as minima on the PES. Experimental values are given in italics. [a] Experimental values from X-ray analysis taken from ref. [24]. [b] Experimental values from X-ray analysis of a substituted analogue taken from ref. [25]. [c] Experimental values from X-ray analysis taken from ref. [21]. [d] Experimental values from X-ray analysis of a substituted analogue taken from ref. [26].

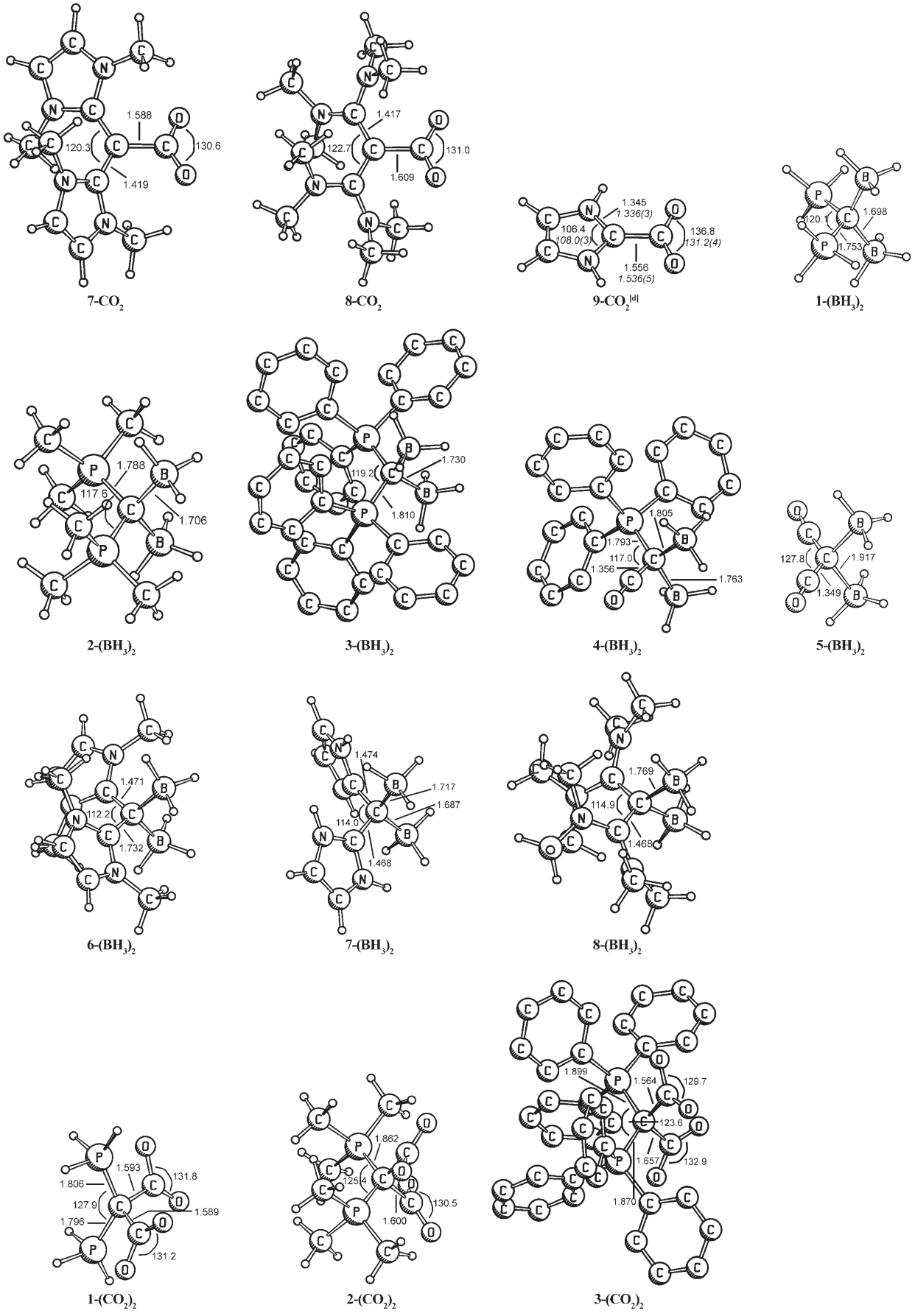

Figure 1. (Continued).

bond lengths of the L_2C–A donor–acceptor bonds are somewhat shorter than the theoretical values. The difference is at least partly due to solid-state effects. Systematic studies of donor–acceptor complexes have shown that the interatomic distances in the solid state are always shorter than in the gas phase.[33] Note that CO_2 adopts a strongly bent geometry in all complexes, where the O-C-O angle varies between 127.7 and 136.8°. The theoretically predicted bending is in agreement with the experimental values for the O-C-O angle in **3-CO$_2$** and **9-CO$_2$**. The experimental data given for **9-CO$_2$** were taken from an X-ray structure analysis of a substituted homologue which has isopropyl substituents at the nitrogen atoms and methyl groups in the 4,5-positions of the imidazol-2-ylidene ring.[26] Note that the plane of the CO_2 ligand in the experimental structure is twisted with respect to the five-membered ring by 69.0(2)°, probably due to the isopropyl substituents. The calculated structure of **9-CO$_2$** has a planar (C_{2v}) geometry.

All compounds **1**–**8**, which can formally be written as divalent carbon(0) compounds CL_2, bind two Lewis acids BH_3 yielding the complexes **N-(BH$_3$)$_2$** (**N** = **1**–**8**) as energy minima. During the geometry optimization of the NHC complex **9-(BH$_3$)$_2$** a rearrangement takes place in which one BH_3 ligand binds to one nitrogen atom of NHC. This finding supports the classification of **9** as a carbene, while **1**–**8** exhibit a divalent carbon(0) behavior. The geometry optimizations of the complexes with two CO_2 ligands **N-(CO$_2$)$_2$** gave minima only for **N** = **1**–**3**, while for the other compounds dissociation of one CO_2 ligand takes place. Figure 1 shows that the R_3P–C and C–CO_2 bonds in **N-(CO$_2$)$_2$** are significantly longer than in **N-CO$_2$**. The energy calculations discussed below indicate that the former species are energetically higher lying than the fragments $(R_3P)_2C$ and $2\,CO_2$. It seems highly unlikely that the **N-(CO$_2$)$_2$** complexes will be synthesized.

The data in Table 1 suggest that the L–C bond lengths in L_2C–H^+ are substantially longer than in neutral CL_2 (see Figure 1 in the preceding paper[1]) except for **9-H$^+$**, for which the N–C bonds in the ring become shorter upon protonation. The latter finding can be explained with enhanced N→C π donation to the protonated carbon atom, which becomes more electron deficient in the cation. Considering the nature of the L→C donor–acceptor bond in the divalent carbon(0) compounds **1**–**8**, the bond lengthening in the protonated complexes is surprising, because the proton should enhance the acceptor ability of the carbon atom in L→(CH$^+$)←L. Longer L–C bonds than in the parent compounds CL_2 are also found in the other complexes L_2C–BH_3 and L_2C–CO_2. The L–C bond lengthening in L_2C–CO_2 may be partly due to steric repulsion between CO_2 and L_2, but where does the clear bond lengthening in L_2C-H^+ come from? Before we address this question, we discuss the calculated bond dissociation energies of the donor–acceptor bonds in L_2C–A and L_2C–A_2 (Table 2).

The calculated protonation energies (PEs) of **1**–**9** suggest that carbodicarbenes **6** and **7** are the strongest bases of the nine carbon compounds, but the PE of TAA **8** is only slightly lower. The calculations at all levels of theory predict that the PE of **8** is higher than those of **1**–**5** and **9**, which is remarkable. The bonding analysis of the parent compounds **1**–**9** showed that the linear TAA has the least carbon lone-pair character, and it is formally written with two C=C double bonds.[1] This is a further hint besides the shallow bending potential[1] that **8** is a "masked" divalent carbon(0) compound. We point out that the order of the first PE is not the same as that of the second PE, which exhibits a significantly different trend. Table 2 shows that the highest second PE is calculated for CDP compound **3**. There is also a much larger substituent effect on the second PE of CDPs **1**–**3** than on the first PE, which indicates that the stabilization of the resulting cation plays an important role, too. The second PE of **2** is much lower (165.2 kcal mol^{-1}) than for **3** (193.4 kcal mol^{-1}), while the first PE of the two compounds is nearly the same. The second PE of NHC **9** (56.6 kcal mol^{-1}) is rather small due to the lower electron density at the central atom. For carbon suboxide (**5**, 23.6 kcal mol^{-1}) the positive second PE is remarkable, since it indicates synthetic accessibility for this dication composed of only seven atoms. Note that the second PE of TAA **8** (158.5 kcal mol^{-1}) is still very high. It is noteworthy that double protonation of a tetraami-

Table 2. Dissociation energies D_e of Lewis acid complexes **1-A** to **9-A** and **1-A$_2$** to **9-A$_2$** with **A** = H^+, BH_3, CO_2. Energies [kcal mol^{-1}] at the BP86 level of theory, with MP2 values in parentheses and SCS-MP2 values in italics. All energies were calculated with the TZVPP basis set. BP86/SVP geometries were employed.

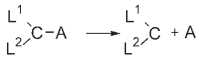

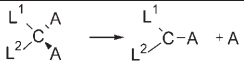

N	N-H$^+$			N-BH$_3$			N-CO$_2$			N-(H$^+$)$_2$			N-(BH$_3$)$_2$			N-(CO$_2$)$_2$		
1	259.4	(262.3)	*265.7*	40.5	(42.8)	*39.1*	13.6	(15.7)	*13.5*	119.2	(120.2)	*123.2*	36.4	(40.6)	*36.4*	−13.6	(−10.7)	*−13.3*
2	285.4	(284.9)	*288.3*	45.2	(49.1)	*44.9*	14.6	(17.6)	*14.7*	165.2	(162.3)	*165.2*	37.9	(44.9)	*39.9*	−11.9	(−7.8)	*−11.6*
3	286.0	(285.6)	*289.7*	32.9	(44.2)	*38.7*	1.3	(12.0)	*7.8*	193.4	(190.9)	*194.3*	23.0	(33.2)	*27.0*	−16.3	(−5.7)	*−10.7*
4	252.5	(252.7)	*257.0*	28.7	(33.0)	*29.8*		–[a]		129.7	(126.5)	*128.9*	11.7	(18.3)	*13.1*		–[a]	
5	181.6	(187.4)	*192.5*	10.0	(11.0)	*8.9*		–[a]		23.6	(34.1)	*37.6*	2.3	(6.6)	*3.3*		–[a]	
6	297.3	(299.9)	*302.6*	64.4	(68.0)	*63.4*		–[b]		155.7	(162.4)	*164.1*	23.5	(33.8)	*28.4*		–[a]	
7	297.5	(302.1)	*304.6*	46.1	(53.6)	*48.3*	13.2	(21.9)	*17.3*	170.3	(175.2)	*178.2*	24.3	(34.0)	*29.4*		–[a]	
8	292.2	(290.8)	*291.8*	37.2	(39.8)	*32.7*	4.3	(8.0)	*2.2*	158.5	(158.1)	*162.2*	9.5	(17.4)	*12.5*		–[a]	
9	259.9	(261.1)	*262.4*	58.6	(57.3)	*53.2*	10.4	(10.7)	*7.8*	56.6	(52.5)	*58.0*		–[c]			–[a]	

[a] Dissociation occurs during optimization. [b] CO_2 deprotonates both NHCs. [c] One BH_3 molecule dissociates and forms a B_2H_6 species with η^1 coordination towards the NHC.

no compound preferentially takes place at a carbon atom formally having two double bonds in the neutral form and not at the nitrogen atom.[34] The theoretical finding is supported by the X-ray analyses of **8-H$^+$**[32] and **8-(H$^+$)$_2$**.[32b] In a previous study we showed that the TAA compound with diethylamino substituents has a second PE which is even about 25 kcal mol^{-1} higher than that of **8**, while the first PE of the ethyl derivative is smaller than that of methyl compound **8**.[5b] The second PE of carbodicarbenes **6** (155.7 kcal mol^{-1}) and **7** (170.3 kcal mol^{-1}) are as expected rather high, but the values are smaller than for CDP **3**.

The generally high bond energies for the BH_3 complexes (Table 2) suggest that all complexes L_2C–BH_3 should be synthetically accessible except **5-BH$_3$**, which has a rather weak bond. Complexes **3-BH$_3$**[24] and a substituted analogue of **9-BH$_3$** which has ethyl substituents at the nitrogen atoms and methyl groups in the 4- and 5-positions of the imidazol-2-ylidene ring[25] are already known, but the bond strength has not been measured. Note that the calculations at the BP86/TZVPP level predict that the CDP complex **3-BH$_3$** has a more weakly bonded ligand ($D_e = 32.9$ kcal mol^{-1}) than the parent system **1-BH$_3$** ($D_e = 40.5$ kcal mol^{-1}), while the MP2 and SCS-MP2 calculations suggest that the CDP-BH_3 bonds in the two complexes have similar BDEs. We think that the latter result is more reliable and that the DFT value is subject to the self-interaction error of the functionals. The calculated energies for **6-BH$_3$** and **9-BH$_3$** indicate that the C→B donor acceptor bonds appear to be stronger than N→Al bonds, which were previously assigned as the strongest donor–acceptor bonds between neutral main group Lewis acids and bases with bond dissociation enthalpy approaching 50 kcal mol^{-1}.[35] Since aluminium compounds are stronger Lewis acids than boron compounds, it can be expected that complexes like **3-AlCl$_3$** and **9-AlCl$_3$** may even be more strongly bonded than **6-BH$_3$** and **9-BH$_3$**. Preliminary calculations support this assumption.[36] Complexes **3-AlBr$_3$**[37] and **9-AlR$_3$** (R = Cl, H, Me with different substitution patterns at the NHC ring)[38,39] have already been isolated and characterized.

The weaker Lewis acid CO_2 yields complexes L_2C-CO_2 which have lower BDEs than L_2C-BH_3 (Table 2). The complex **3-CO$_2$** has a theoretically predicted BDE at the SCS-MP2/TZVPP level of only $D_e = 7.8$ kcal mol^{-1}, which drops to $D_0 = 6.1$ kcal mol^{-1} when zero-point vibrational energy contributions are considered. The BP86/TZVPP value is even smaller ($D_e = 1.3$ kcal mol^{-1}, $D_0 = -0.4$ kcal mol^{-1}). The calculated data thus indicate that **3-CO$_2$** is only marginally stable, but the complex could be isolated in the solid state and its X-ray structure analysis has been published.[21] It appears that the intermolecular forces in solid **3-CO$_2$** enhance the stability of the compound, which dissociates in the gas phase into **3** and CO_2. A similar situation exists for **9-CO$_2$**, which at the SCS-MP2/TZVPP level is calculated to have the same BDE as **3-CO$_2$** ($D_e = 7.8$ kcal mol^{-1}). A substituted homologue of the latter complex which has isopropyl substituents at the nitrogen atoms and methyl groups at the 4,5-positions of the imidazol-2-ylidene ring could also be isolated, and an X-ray structure is available.[26] Interestingly, the BP86/TZVPP BDE of **9-CO$_2$** is slightly larger ($D_e = 10.4$ kcal mol^{-1}) than the SCS-MP2/TZVPP value, while for complex **3-CO$_2$** the BP86/TZVPP value ($D_e = 1.3$ kcal mol^{-1}) is significantly smaller than that at the SCS-MP2/TZVPP level. We think that the SCS-MP2/TZVPP energies are more reliable for the same reasons as given above. Fortunately, the BDE values at the BP86/TZVPP and SCS-MP2/TZVPP levels for the other complexes generally agree quite well. Both methods predict that carbodicarbene complex **7-CO$_2$** should be stable enough to be isolated in a condensed phase. The geometry optimization of **6-CO$_2$** yields a structure in which the CO_2 ligand has deprotonated the NH groups of the NHC rings.

The calculated bond energies for the second BH_3 ligand of CDP complexes **1-(BH$_3$)$_2$**, **2-(BH$_3$)$_2$**, and **3-(BH$_3$)$_2$** and carbodicarbene complexes **6-(BH$_3$)$_2$** and **7-(BH$_3$)$_2$** are still quite high, while the BDE values for **4-(BH$_3$)$_2$**, **5-(BH$_3$)$_2$**, and **8-(BH$_3$)$_2$** are rather small. The geometry optimization of **9-(BH$_3$)$_2$** leads to a structure in which the second boron atom binds via a B-H-B bridge to the first BH_3 molecule and loses contact to the NHC ring. Experimental studies aimed at isolating **3-(BH$_3$)$_2$** resulted in ionic complex [{(μ-H)H_4B_2}C(PPh_3)$_2$](B_2H_7). The X-ray analysis showed that it has two boron–carbon donor–acceptor bonds between the C(PPh_3)$_2$ donor species and the $[B_2H_5]^+$ acceptor moiety, which has a B-H-B bridge.[24] As mentioned above, the complexes **N-(CO$_2$)$_2$** (**N** = **1**–**3**) have negative bond dissociation energies, that is, bond dissociation is an exothermic process. The optimized structures are local minima on the respective potential-energy surfaces (PES) which are unlikely to be observed under normal conditions.

We return to the question why the L→CH$^+$ donor–acceptor bonds in protonated species **1-H$^+$**–**8-H$^+$** have clearly longer interatomic distances than the L→C bonds in neutral **1**–**8**, although the binding interactions in the cations can be expected to be much stronger than in the neutral molecules. Table 3 gives the calculated bond dissociation energies for the reaction $L_2CH^+ \rightarrow L_2 + CH^+$. We also calculated the BDE for **9-H$^+$** yielding HN=CH–CH=NH + CH$^+$ as products. Comparison of the calculated BDEs of the latter reactions with the data for the neutral species L_2C (**1**–**9**; see Table 2 in the preceding paper[1]) clearly shows that the cations have much higher BDEs than the neutral compounds. The strongest bonds in both series are calculated for compounds **8** > **7** > **6** and **8-H$^+$** > **7-H$^+$** > **6-H$^+$**, although the trend of the BDE values is not exactly the same for the cations as for the neutral compounds. But why are the much stronger C–L bonds in **1-H$^+$**–**8-H$^+$** significantly longer than in **1**–**8**?

To investigate the difference between the donor–acceptor interactions in the neutral and charged systems we performed an EDA on the parent system **1-H$^+$** and compared the results with the data for **1** (Table 4). The acceptor moiety in $(H_3P)_2$-CH$^+$ is the cation CH$^+$, which has a $^1\Sigma^+$ ground state (Figure 2a). This state is not the electronic reference state of the molecule, because **1-H$^+$** has a π-electron

Table 3. Dissociation energies D_e, ZPE-corrected energies D_0 and energies including thermal and vibrational contributions D_0^{298} for the dissociation reaction $H^+–C(L^1L^2)\rightarrow CH^+ + L^1 + L^2$. All energies [kcal mol^{-1}] calculated with the TZVPP basis set. BP86/SVP geometries were employed.

			BP86		MP2		SCS-MP2	
L^1	L^2	No.	D_e	D_0^{298}	D_e	D_0^{298}	D_e	D_0^{298}
PH_3	PH_3	**1-H$^+$**	222.6	214.5	225.0	217.0	214.6	206.6
PMe_3	PMe_3	**2-H$^+$**	276.5	269.6	284.1	277.2	271.2	264.3
PPh_3	PPh_3	**3-H$^+$**	271.1	265.0	290.9	284.8	275.6	269.5
PPh_3	CO	**4-H$^+$**	269.5	263.2	263.3	257.0	250.6	244.3
CO	CO	**5-H$^+$**	212.6	205.7	196.2	189.3	183.1	176.2
NHC_H	NHC_H	**6-H$^+$**	331.0	323.2	328.5	320.8	316.6	308.9
NHC_{Me}	NHC_{Me}	**7-H$^+$**	331.7	323.2	337.5	329.0	323.2	314.7
$C(NMe_2)_2$	$C(NMe_2)_2$	**8-H$^+$**	350.3	340.4	364.0	354.0	348.0	338.0
HN=CH–CH=NH		**9-H$^+$**	287.0	279.4	285.5	277.9	272.2	264.6

Table 4. EDA (BP86/TZ2P) results [kcal mol^{-1}] and calculated C–P bond lengths [Å] for $[HC(PH_3)_2]^+$ (**1-H$^+$**)and $[C(PH_3)_2]$ (**1**). The interacting fragments for $[HC(PH_3)_2]^+$ are CH^+ ($^1\Delta$) and $(PH_3)_2$. The interacting fragments for **1** are C (^{1}D, $s^0p_\sigma^2p_{\pi\perp}{}^2p_{\pi\parallel}{}^0$) and $(PH_3)_2$.[a]

	$CH^+–(PH_3)_2$		$C–(PH_3)_2$	
ΔE_{int}	−398.8		−552.4	
ΔE_{Pauli}	334.9		204.2	
ΔE_{elstat}[b]	−137.1	(18.7)	−203.9	(26.9)
ΔE_{orb}[b]	−596.6	(81.3)	−552.7	(73.1)
$\Delta E_\sigma(a_1)$[c]	−316.1	(53.0)	−300.9	(54.4)
$\Delta E_\delta(a_2)$[c]	−4.6	(0.8)	−1.2	(0.2)
$\Delta E_{\pi\perp}(b_1)$[c]	−33.9	(5.7)	−73.7	(13.3)
$\Delta E_{\pi\parallel}(b_2)$[c]	−242.0	(40.6)	−176.9	(32.0)
ΔE_{prep}	180.3		448.2	
ΔE_{prep} (CH^+/C)	155.3		427.8	
ΔE_{prep} $(PH_3)_2$	25.0		20.4	
ΔE ($=-D_e$)	−218.6		−104.3	
d(C–P)	1.720		1.654	

[a] The data are taken from the preceding paper,[1] Table 5, fragmentation scheme (d). [b] The values in parentheses are the percentage contributions to the total attractive interactions $\Delta E_{elstat} + \Delta E_{orb}$. [c] The values in parentheses are the percentage contributions to the total orbital interactions ΔE_{orb}.

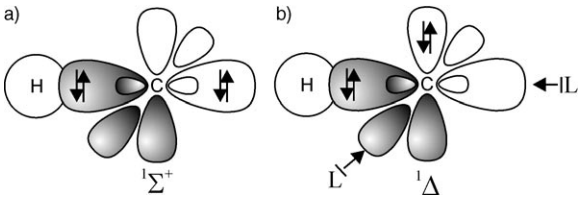

Figure 2. Schematic representation of the bonding situation in CH^+ a) in the $^1\Sigma^+$ ground state and b) in the $^1\Delta$ excited state which is the reference state for the $L_2\rightarrow CH^+$ donor–acceptor interactions.

lone pair at the carbon atom while both p(π) orbitals of CH^+ are empty. The lowest lying electronic state which has an occupied π lone pair is the $^1\Delta$ state (Figure 2b). This state is calculated at the BP86/TZ2P level to be 155.3 kcal mol^{-1} higher in energy than the $^1\Sigma^+$ ground state, which is in very good agreement[40] with the experimental value of 150.4 kcal mol^{-1}.[41]

The EDA data in Table 4 are given for the interactions between $(PH_3)_2$ in the electronic ground state and CH^+ ($^1\Delta$) in the cation **1-H$^+$**. An NBO analysis of **1** and **1-H$^+$** suggests that the hybridization at the carbon end of the C–P bond is $sp^{2.5}$ for **1** and $sp^{2.0}$ for **1-H$^+$**. The larger percentage contribution of the 2s orbital in the latter species does not explain the longer C–P bond. An explanation can be given when the EDA results of **1-H$^+$** are compared with the EDA values for **1**, which are also listed in Table 4. Note that the instantaneous interaction energy of **1-H$^+$** ($\Delta E_{int} = -398.8$ kcal mol^{-1}) is clearly lower than in **1** ($\Delta E_{int} = -552.4$ kcal mol^{-1}), but the latter compound has a smaller BDE. This is because the preparation energy ΔE_{prep} of **1** is much higher ($\Delta E_{prep} = 448.2$ kcal mol^{-1}) than that of **1-H$^+$** ($\Delta E_{prep} = 180.3$ kcal mol^{-1}). The breakdown of the ΔE_{int} values into the attractive contributions of the electrostatic interaction ΔE_{elstat} and orbital interactions ΔE_{orb} reveals that the nature of the chemical bonding in the two compounds is not very different. The orbital interactions in **1-H$^+$** are slightly stronger ($\Delta E_{orb} = -596.6$ kcal mol^{-1}) than in **1** ($\Delta E_{orb} = -552.7$ kcal mol^{-1}) because the acceptor orbitals in the positively charged moiety are energetically much lower lying than those in the neutral compound. This yields stronger orbital interactions even at a larger distance. The crucial difference between the EDA results of the two compounds lies in the calculated Pauli repulsion, which is much stronger in **1-H$^+$** ($\Delta E_{Pauli} = 334.9$ kcal mol^{-1}) than in **1** ($\Delta E_{Pauli} = 204.2$ kcal mol^{-1}), although the former has a longer bond. The earlier onset of Pauli repulsion when the ligands approach CH^+ rather than a naked carbon atom can be explained with the help of Figure 2b. One ligand donates electronic charge into the empty p orbital of CH^+. The other ligand L donates electronic charge into an empty sp hybrid but it encounters Pauli repulsion from the electron pair in the backside lobe of the C–H$^+$ bonding orbital, which is missing when the ligands approach a naked carbon atom (see Figure 6a in Part 1). The stronger Pauli repulsion in **1-H$^+$** at longer distances explains why the C–L bonds in the cation are longer than in **1**. Therefore, the electrostatic attraction in **1-H$^+$** is clearly weaker ($\Delta E_{elstat} = -137.1$ kcal mol^{-1}) than in **1** ($\Delta E_{elstat} = -234.4$ kcal mol^{-1}). The electrostatic interaction comes mainly from the attraction between the phosphorous lone-pair electrons and the carbon nucleus, which is weaker in **1-H$^+$** than in **1** because the P–C interatomic distance is longer.[42] The higher BDE of **1-H$^+$** then comes from the significantly smaller preparation energy.

The calculated bond lengths and bond energies for **1-H$^+$** and **1** clearly show that the strength of a bond is not directly related to the overlap of the orbitals, as is frequently assumed, but that the Pauli repulsion plays an important role. In a recent systematic investigation of the nature of the covalent bond, it was shown that avoiding overlap between doubly occupied orbitals, which is prohibited by the Pauli postulate, is a very important factor in determining the equi-

librium distance of a chemical bond.[43] It is not true that the maximum bond strength of a covalent bond is achieved at the maximum value of the overlap integral. It is the interplay between attractive (ΔE_{orb}) and repulsive (ΔE_{Pauli}) electron–electron interactions which determines the strength and length of the bond. A positive charge at the acceptor moiety enhances the attraction, because the acceptor orbital is energetically lower lying, while at the same time the repulsion at longer distances is reduced due to the orbital contraction in the cation. A similar situation was recently reported for the interactions between the neutral and charged Lewis acids BH_3 and BH_2^+ with CO. The H_2B^+–CO bond is longer but stronger than the H_3B–CO bond.[44,45]

Illuminating information about the electronic structures of the complexes L_2C–A and L_2C–A_2 (A = H^+, BH_3 and CO_2) is provided by the calculated partial charges, which are given together with those of parent compounds **1**–**9** in Table 5. In most compounds, protonation of the carbon donor atom leads to a slightly less negatively charged C donor atom compared to the neutral compounds, while the carbene carbon atom in **9-H$^+$** is a little more positively charged than in **9**. Surprisingly, the central carbon atom in **5-H$^+$**, **7-H$^+$**, and **8-H$^+$** carries a higher negative charge than in the neutral compound. This is particularly striking for TAA **8**, in which the negative charge in the neutral compound (−0.21 e) increases to −0.47 e in the C-protonated species **8-H$^+$**. The counterintuitive increase in negative charge of an atom after protonation suggests that the "hidden" divalent carbon(0) character of **8** comes to the fore on protonation at the carbon atom. Note that the partial charge at the central carbon atom in **8-H$^+$** has a similar value to those in the protonated carbodicarbenes **6-H$^+$** (−0.46 e) and **7-H$^+$**(−0.52 e). The higher negative charges at the central carbon atom of **5-H$^+$**, **7-H$^+$**, and **8-H$^+$** come from the enhanced charge donation $L_2C\rightarrow C(H^+)\leftarrow CL_2$, which more than compensates for the charge flow to the proton $(L_2C)C\rightarrow H^+$. A similar observation can be made for the other complexes L_2C-BH_3 and L_2C-CO_2, where the negative charges at the carbon donor atom in **8-BH$_3$** and **8-CO$_2$** are clearly higher than in **8**, while a slightly smaller negative charge is calculated for the other species **N-BH$_3$** and **N-CO$_2$** compared with **N** (**N** = **1**–**7**), except for **5-BH$_3$**, in which the negative charge at C is nearly the same as in **5**. The carbene donor atom in protonated NHC **9-H$^+$** and in the complexes **9-BH$_3$** and **9-CO$_2$** sticks out because it is the only donor atom which remains positively charged although the total charge of the donor molecule $q(CL_2)$ in **9-A** is very similar to the charges $q(CL_2)$ in the other complexes **N-A** (**N** = **1**–**8**). The partial charge q(C) in **9-A** is slightly larger than in neutral **9** (Table 5).

Further information comes from the calculated partial charges in the doubly protonated species **N-(H$^+$)$_2$** (**N** = **1**–**9**) and in **N-(BH$_3$)$_2$** (**N** = **1**–**8**), which also exhibit surprising features (Table 5). All tetracoordinate carbon donor atoms carry a negative partial charge even in the dications. The second protonation yields only slightly less negatively charged carbon donor atoms in **1-(H$^+$)$_2$** to **4-(H$^+$)$_2$** compared with the monocations but the carbon donor atoms in the dications **5-(H$^+$)$_2$** to **9-(H$^+$)$_2$** are more negatively charged than in the respective monocations. The change in partial charge from cation to dication is particularly striking for doubly protonated NHC **9-(H$^+$)$_2$**, in which the second protonation turns the positively charged carbon atom into a negatively charged species. The change of the atomic partial charges at the carbon atom after complexation by H^+, BH_3 or CO_2 surely turns common wisdom and chemical intuition upside down. The mind-boggling partial charges can be understood when the bonding situation of divalent carbon(0) compounds is considered.

The difference between the carbon–ligand donor–acceptor bond of the divalent carbon(0) complex **1-BH$_3$** and that of the carbon(II) complex **9-BH$_3$** is also revealed by the topological analysis of the electron-density distribution, which was performed in the framework of the AIM method.[13] Figure 3 shows the contour line diagrams of the Laplacian $\nabla^2\rho(r)$ of the two molecules in the plane of the donor molecules (left) and in the perpendicular plane (right). The former views show in both molecules for the C–B bonds a region of charge concentration ($\nabla^2\rho(r)<0$, solid lines) at the carbon donor atom which points toward the electron-de-

Table 5. NBO partial charges (BP86/TZVPP//BP86/SVP) for parent compounds **N** and the complexes **N-H$^+$**, **N-BH$_3$**, **N-CO$_2$**, **N-(H$^+$)$_2$**,**N-(BH$_3$)$_2$** and **N-(CO$_2$)$_2$** (**N** = **1**–**9**). Atomic partial charges [e] are given for the central carbon atom [q(C)] and the whole CL_2-fragment [$q(CL_2)$].


			N	**N-H$^+$**		**N-BH$_3$**		**N-CO$_2$**		**N-(H$^+$)$_2$**		**N-(BH$_3$)$_2$**		**N-(CO$_2$)$_2$**	
N	L^1	L^2	q(C)	q(C)	$q(CL_2)$	q(C)	$q(CL_2)$	q(C)	$q(CL_2)$	q(C)	$q(CL_2)$	q(C)	$q(CL_2)$	q(C)	q(CL_2)
1	PH_3	PH_3	−1.32	−1.26	+0.68	−1.20	+0.48	−1.11	+0.57	−1.01	+1.32	−1.04	+0.89	−0.90	+0.89
2	PMe_3	PMe_3	−1.47	−1.36	+0.70	−1.34	+0.53	−1.22	+0.73	−1.07	+1.39	−1.12	+0.99	−0.88	+1.13
3	PPh_3	PPh_3	−1.43	−1.33	+0.70	−1.30	+0.48	−1.14	+0.61	−1.07	+1.41	−1.11	−0.89	−0.86	+1.14
4	PPh_3	CO	−0.96	−0.91	+0.68	−0.86	+0.45	–[a]		−0.88	+1.29	−0.84	+0.72	–[a]	
5	CO	CO	−0.55	−0.67	+0.62	−0.56	+0.31	–[a]		−0.74	+1.10	−0.60	+0.47	–[a]	
6	NHC_H	NHC_H	−0.51	−0.46	+0.75	−0.36	+0.56	–[b]		−0.52	+1.41	−0.50	+0.98	–[a]	
7	NHC_{Me}	NHC_{Me}	−0.50	−0.52	+0.75	−0.40	+0.55	−0.42	+0.70	−0.53	+1.42	−0.50	+0.92	–[a]	
8	$C(NMe_2)_2$	$C(NMe_2)_2$	−0.21	−0.47	+0.76	−0.36	+0.55	−0.37	+0.70	−0.51	+1.51	−0.49	+0.84	–[a]	
9	HN=CH–CH=NH		+0.04	+0.20	+0.73	+0.32	+0.50	+0.30	+0.64	−0.14	+1.29	–[c]	0.00	–[a]	

[a] Dissociation occurs during optimization. [b] CO_2 deprotonates both NHCs. [c] One BH_3 molecule dissociates and forms a B_2H_6 species with η^1 coordination towards the NHC moiety.

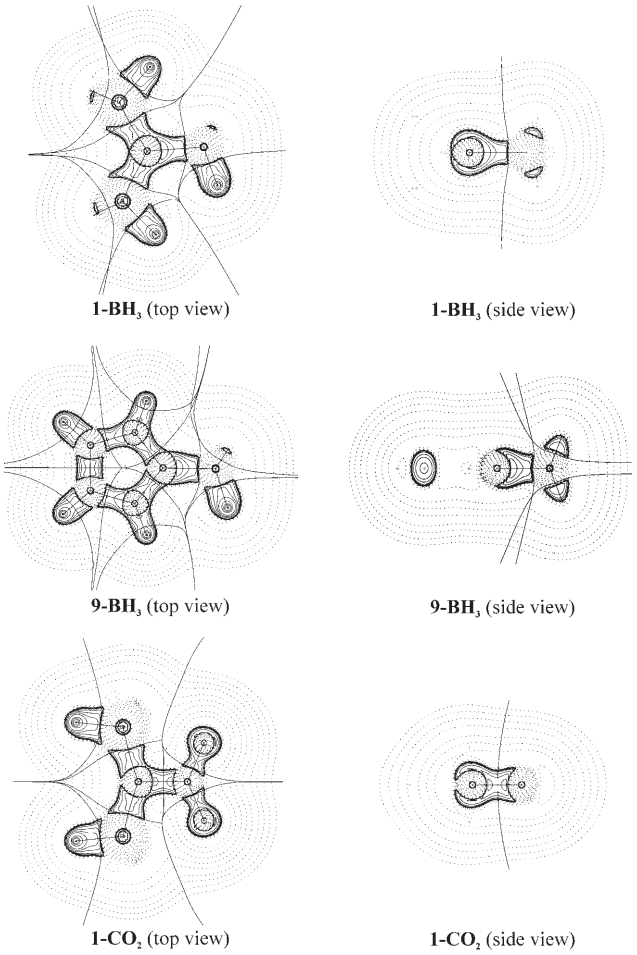

Figure 3. Contour line diagrams $\nabla^2\rho(r)$ of the complexes **1-BH$_3$**, **9-BH$_3$**, and **1-CO$_2$** in two different views. Solid lines indicate areas of charge concentration ($\nabla^2\rho(r)<0$) while dashed lines show areas of charge depletion ($\nabla^2\rho(r)>0$). The thick solid lines connecting the atomic nuclei are the bond paths. The thick solid lines separating the atomic basins indicate the zero-flux surfaces crossing the molecular plane.

ficient boron atom. The difference between the molecules comes to the fore when the shape of the Laplacian at the carbon atom in the perpendicular plane is considered. The carbon donor atom of **1-BH$_3$** still has a nearly spherical area of charge concentration which clearly extends in the π direction. This charge concentration in the π direction is missing in **9-BH$_3$**. This finding nicely explains why **1-BH$_3$** can still serve as a donor for a second Lewis acid. The Laplacian distribution at the carbon atom of the complex **1-CO$_2$**, which is also shown in Figure 3, exhibits a similar charge concentration in the π direction as **1-BH$_3$**.

We analyzed the nature of the donor–acceptor bonds of the equilibrium structures of L_2C–BH_3, L_2C–CO_2 and L_2C–$(BH_3)_2$ with the EDA method. Table 6 gives the results for selected complexes **N-BH$_3$**, **N-(BH$_3$)$_2$** and **N-CO$_2$**. The results for the remaining structures are not presented here because they do not give further insight into the bonding situation.

The EDA results for the complexes **N-BH$_3$** suggest that the C→BH_3 donor–acceptor bonds mainly comes from the interaction of the carbon σ lone pair, which gives rise to strong electrostatic attraction due to overlap with the boron nucleus (ΔE_{elstat}). The carbon σ lone-pair orbital also yields a covalent σ bond by overlapping with the σ LUMO of BH_3 (ΔE_σ). Note that carbodicarbene **6** has a significantly higher interaction energy with BH_3 ($\Delta E_{int}=-91.1$ kcal mol^{-1}) than NHC **9** ($\Delta E_{int}=-77.3$ kcal mol^{-1}), although the complex **9-BH$_3$** has a shorter B–C bond (1.582 Å) than **6-BH$_3$** (1.643 Å). Here the stronger bond comes from the attractive terms ΔE_{elstat} and ΔE_{orb}, which in the latter complex are clearly larger than in the former. The stronger attraction in **6-BH$_3$** is nearly compensated by the larger preparation energy ΔE_{prep} compared with **9-BH$_3$**, which leads to an only slightly larger BDE for the complex **6-BH$_3$**. The interaction energies between the Lewis bases **1** and **6** and two BH_3 mol-

Table 6. EDA (BP86/TZ2P) results [kcal mol^{-1}] of selected BH_3 and CO_2 complexes of **N** (**N**=**1**, **5**, **6**, **9**). The adducts **N-BH$_3$** were optimized under C_s symmetry constraints, and adducts **N-(BH$_3$)$_2$** and **N-CO$_2$** under C_{2v} symmetry constraints. The interacting fragments are **N** and the Lewis acids **A**=BH_3, $(BH_3)_2$ and CO_2.

	N-BH$_3$				N-(BH$_3$)$_2$			N-CO$_2$	
	1-BH$_3$	**5-BH$_3$**	**6-BH$_3$**	**9-BH$_3$**	**1-(BH$_3$)$_2$**	**5-(BH$_3$)$_2$**	**6-(BH$_3$)$_2$**	**1-CO$_2$**	**9-CO$_2$**
ΔE_{int}	−53.4	−21.0	−91.1	−77.3	−121.7	−27.9	−172.8	−70.9	−53.0
ΔE_{Pauli}	112.8	75.4	168.3	160.4	284.5	115.6	342.3	478.9	358.0
ΔE_{elstat}[a]	−72.6 (43.7)	−35.8 (37.2)	−127.6 (49.2)	−118.1 (49.7)	−185.4 (45.6)	−56.6 (39.4)	−235.2 (45.7)	−236.9 (43.1)	−199.3 (48.5)
ΔE_{orb}[a]	−93.6 (56.3)	−60.6 (62.8)	−131.7 (50.8)	−119.6 (50.3)	−220.9 (54.4)	−86.9 (60.6)	−279.9 (54.3)	−312.9 (56.9)	−211.7 (51.5)
$\Delta E_\sigma(a')$[b]	−87.8 (93.8)	−57.5 (94.9)	−123.0 (93.4)	−108.3 (90.6)					
$\Delta E_\pi(a'')$[b]	−5.8 (6.2)	−3.1 (5.1)	−8.7 (6.6)	−11.3 (9.4)					
$\Delta E_\sigma(a_1)$[b]					−94.6 (42.8)	−37.8 (43.6)	−118.3 (42.2)	−261.0 (83.4)	−187.5 (88.5)
$\Delta E_\delta(a_2)$[b]					−8.1 (3.7)	−5.8 (6.7)	−3.5 (1.3)	−3.2 (1.0)	−1.6 (0.8)
$\Delta E_{\pi\perp}(b_1)$[b]					−110.0 (49.8)	−41.0 (47.2)	−151.7 (54.2)	−25.7 (8.2)	−13.2 (6.2)
$\Delta E_{\pi\parallel}(b_2)$[b]					−8.3 (3.7)	−2.2 (2.6)	−6.4 (2.3)	−23.1 (7.4)	−9.5 (4.5)
ΔE_{prep}	18.5	11.9	29.6	19.3	46.4	17.6	86.2	61.1	42.8
ΔE_{prep} (N)	1.5	3.9	5.4	0.9	8.2	5.6	37.9	13.0	4.0
ΔE_{prep} (A)	17.0	8.0	24.2	18.4	38.1	12.0	48.3	48.1	38.8
ΔE ($=-D_e$)	−34.8	−9.0	−61.4	−57.9	−75.4	−10.3	−86.6	−9.8	−10.2
d(N–A) [Å]	1.709	1.820	1.643	1.582	1.741	1.984	1.693	1.476	1.548

[a] The values in parentheses are the percentage contributions to the total attractive interactions $\Delta E_{elstat}+\Delta E_{orb}$. [b] The values in parentheses are the percentage contribution to the total orbital interactions ΔE_{orb}.

ecules are roughly twice as high as the ΔE_{int} values for **1-BH_3** and **6-BH_3**, while **5-$(BH_3)_2$** has only a slightly larger interaction energy than **5-BH_3** (Table 6). The EDA data indicate that bent carbon suboxide (**5**) is an intrinsically much weaker donor than **1** and **6**. We note out that the p(π) lone-pair orbital of the divalent carbon(0) donor in the dicoordinate complexes makes a stronger contribution to the attractive orbital term ΔE_{orb} than the p(σ) orbital (cf. the $\Delta E_{\pi\perp}$ values for **N-$(BH_3)_2$**). The two C→BH_3 donor–acceptor bonds are of course degenerate, but the p(π) lone-pair orbital of the donor moiety is more strongly stabilized due to mixing with the 2s AO of carbon during bond formation than the p(σ) lone-pair orbital. Noteworthy is the much larger preparation energy ΔE_{prep} of **6-$(BH_3)_2$** in comparison to **5-$(BH_3)_2$**, which diminishes the difference between the interaction energies and yields less discriminative BDEs.

The EDA results for complexes **1-CO_2** and **9-CO_2** clearly show (Table 6) that CO_2 is an intrinsically strong Lewis acid which engages in even stronger attractive interactions in CDP complex **1-CO_2** ($\Delta E_{int} = -70.9$ kcal mol^{-1}) than in **1-BH_3** ($\Delta E_{int} = -53.4$ kcal mol^{-1}). The reason for the significantly lower BDEs lies in the large preparation energy which is necessary to distort linear CO_2 to a strongly bent geometry in the complexes. The absolute values for the energy terms in the **N-CO_2** bonds are much higher than in **N-BH_3** because the bond is shorter, but the nature of the donor–acceptor bonds, which is given by the percentage contributions of the electrostatic and orbital interactions, is nearly the same in both complexes. Note that the double-bond character of the C–C bonds in **1-CO_2** and **9-CO_2** is very small.[46] The percentage contributions of $\Delta E_{\pi\perp}$ to the total orbital interactions are less than 9% (Table 6).

Transition metal complexes with divalent carbon(0) compounds as ligands: We theoretically investigated the transition metal complexes **N-W(CO)$_5$**, **N-Ni(CO)$_3$**, and **N-Ni(CO)$_2$**. Figure 4 shows the optimized geometries of the molecules at the BP86/SVP level together with the most important bond lengths and angles. The full set of geometrical data is given in Table S1 in the Supporting Information. The calculated BDEs of the L_2C-M(CO)$_n$ bonds at the BP86/TZVPP//BP86/SVP level are also given. We did not calculate the bond energies at the MP2 level because it is well known that the values are not reliable and that spin-component scaling does not fully correct for the inherent MP2 problem.[47]

Figure 4 also gives experimental bond lengths and bond angles of **3-Ni(CO)$_3$**,[23] **3-Ni(CO)$_2$**[23] and substituted analogues of **9-W(CO)$_5$**,[48] **9-Ni(CO)$_3$**[49] and **9-Ni(CO)$_2$**,[49] which are the only species for which experimental data are known to us. The agreement between theory and experiment is very good. Note that the optimized geometry of **9-Ni(CO)$_2$** has an NHC ligand which is orthogonal to the plane of the Ni(CO)$_2$ moiety (C_{2v} symmetry), which agrees with the X-ray structure analysis of an *N*-substituted homologue.[49] The calculated data for the other compounds may thus serve as a reliable prediction for future measurements. The theoretical data show that the L–C bonds in the complexes L_2C–M(CO)$_n$ are longer than in free L_2C except for the N–C bond of the NHC ligand (cf. Figure 1 in the preceding paper in this issue[1]). The same trend was observed for the main group complexes of **1**–**8** with the Lewis acids H^+, BH_3 and CO_2. The calculated C→Ni bonds in the 18-electron complexes **N-Ni(CO)$_3$** are always longer than in the complexes **N-Ni(CO)$_2$**, which are formally 16-electron complexes if the ligands **N** are considered to be two-electron donors. It will be interesting to see if the CL_2 ligands employ both electron lone pairs for the C–Ni bonds in the latter species, which would explain the shorter and stronger bonds. Note that the C_3O_2 ligand changes its coordination mode from η^1 in **5-Ni(CO)$_3$** to η^2 in **5-Ni(CO)$_2$**.

The calculated BDEs shown in Figure 4 indicate that the L_2C–W bonds in **N-W(CO)$_5$** have a similar strength to the L_2C–B bonds in **N-BH_3** (Table 2). The strongest bond is found for **6-W(CO)$_5$** ($D_e = 55.8$ kcal mol^{-1}) and the weakest bond is calculated for **5-W(CO)$_5$** ($D_e = 15.4$ kcal mol^{-1}). The BDE values for **N-W(CO)$_5$** can be compared with the calculated result for W(CO)$_6$ ($D_e = 44.5$ kcal mol^{-1}) obtained at the same level of theory. The latter value gives a theoretical BDE of $D_0^{298} = 43.0$ kcal mol^{-1} after correction for thermal and ZPE contributions, which is in excellent agreement with the experimental value of (46 ± 2) kcal mol^{-1}.[50] The data suggest that the ligands **6** and **9** yield stronger bonds with W(CO)$_5$ than CO, while the other carbon-donor ligands have weaker bonds. The calculated BDE for **3-W(CO)$_5$** ($D_e = 24.4$ kcal mol^{-1}) may be too small for the same reasons discussed above. It is noteworthy that the synthesis of **3-W(CO)$_5$** was reported more than 30 years ago by Kaska et al.,[51] but attempts to obtain crystals which are suitable for X-ray diffraction analysis were unsuccessful.[51,52] The very high basicity of the divalent carbon(0) compounds will easily lead to side reactions, particularly in protic solvents, but the development of experimental methods in the last three decades may eventually lead to the isolation of complexes **N-W(CO)$_5$** (**N** = **1**–**8**). The synthesis of **5-W(CO)$_5$** and **5-Ni(CO)$_3$** would realize a new binding mode of carbon suboxide which has not been observed so far.

The calculated BDEs for **N-Ni(CO)$_3$** and **N-Ni(CO)$_2$** suggest that the L_2C–Ni bonds are weaker than the respective L_2C–W bonds and that the L_2C–Ni(CO)$_2$ bonds are always stronger than the particular L_2C–Ni(CO)$_3$ bond (Figure 4). The theoretically predicted trend of the bond energies is thus L_2C-W(CO)$_5$ > L_2C-Ni(CO)$_2$ > L_2C-Ni(CO)$_3$. The calculated bond energies for **9-Ni(CO)$_3$** and **9-Ni(CO)$_2$** can be compared with experimentally estimated values for *N*-substituted analogues that were recently published by Nolan et al.[49] The bond strengths of the NHC_{Ad}-Ni(CO)$_2$ (Ad = adamantyl) and NHC_{tBu}-Ni(CO)$_2$ complexes were given as 42 and 37 kcal mol^{-1}, respectively. This is in very good agreement with the value $D_0^{298} = 41.7$ kcal mol^{-1} which is calculated for the parent system **9-Ni(CO)$_2$**. The theoretical value for **9-Ni(CO)$_3$** of $D_0^{298} = 34.7$ kcal mol^{-1} is somewhat larger than the experimental estimate of $D_0^{298}(NHC_{Mes}\text{–}Ni(CO)_3) \geq 24$ kcal mol$^{-1} \geq D_0^{298}(NHC_{Ad}\text{–}Ni(CO)_3)$ (Mes = mesityl), but

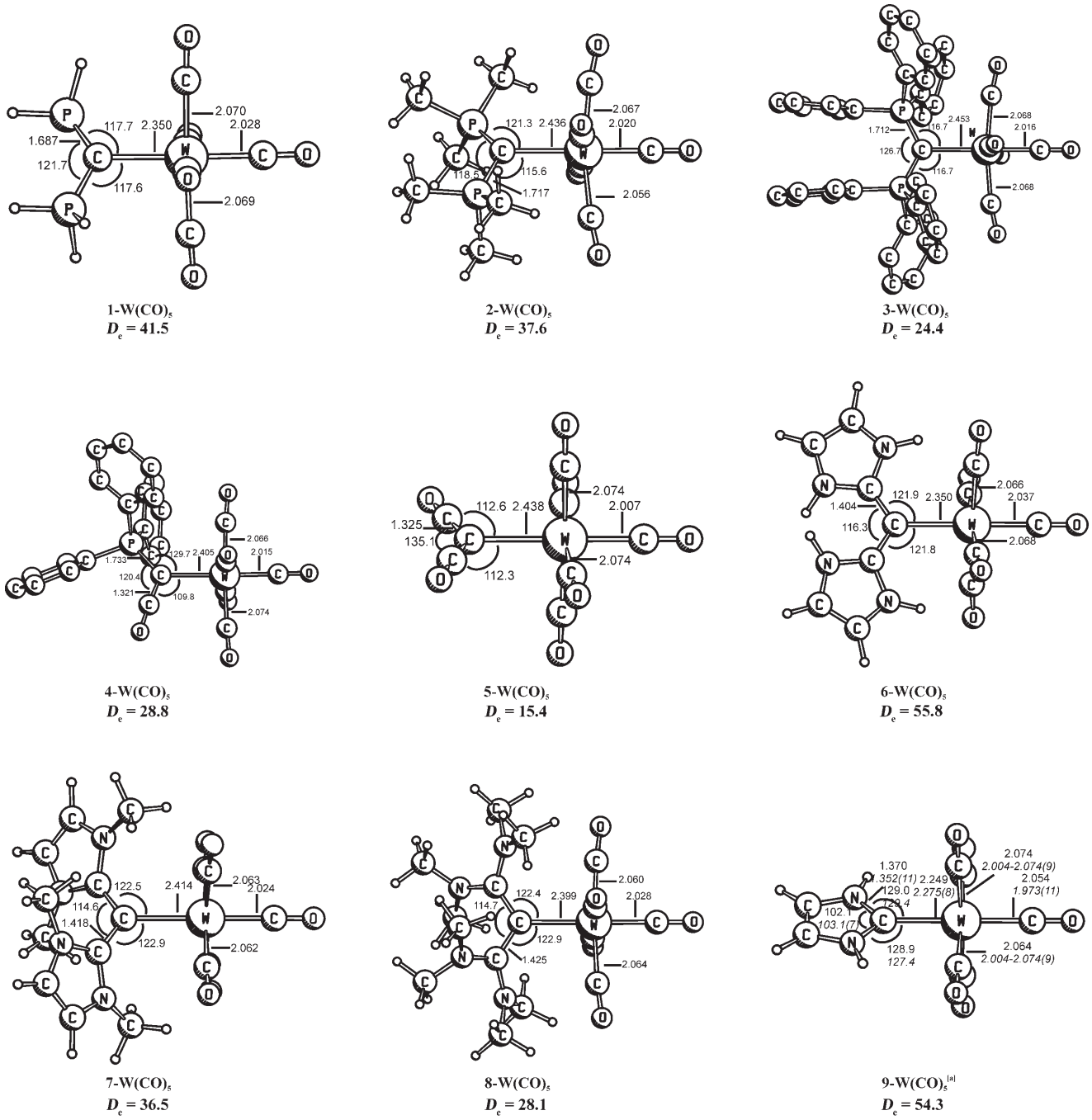

Figure 4. Optimized geometries (bond lengths [Å] and angles [°]) at the BP86/SVP level of **N-W(CO)$_5$**, **N-Ni(CO)$_3$**, and **N-Ni(CO)$_2$** (**N** = **1**–**9**) which were found as minima on the PES. Experimental values are given in italics. Hydrogen atoms of the phenyl rings are omitted for clarity. [a] Experimental values from X-ray analysis taken from ref. [48]. [b] Experimental values from X-ray analysis taken from ref. [23]. [c] Experimental values from X-ray analysis of a substituted analogue taken from ref. [49]. [d] Experimental values from X-ray analysis taken from ref. [23]. [e] Experimental values from X-ray analysis of a substituted analogue taken from ref. [49]. Bond dissociation energies D_e for the N–M bond are given in kcal mol^{-1} at the BP86/TZVPP//BP86/SVP level of theory.

the difference may partly be caused by the bulky substituents.

Table 7 gives the atomic partial charges for the transition metal complexes **N-W(CO)$_5$**, **N-Ni(CO)$_3$**, and **N-Ni(CO)$_2$**. It becomes obvious that the carbon donor atom retains its negative partial charge in **1-TM(CO)$_n$** to **8-TM(CO)$_n$**, which even becomes slightly more negative in the complexes compared with the free ligands (Table 5). This can be explained by the enhanced charge donation $L_2 \rightarrow C$, which compensates for the $L_2C \rightarrow M(CO)_n$ donation. The overall partial charges

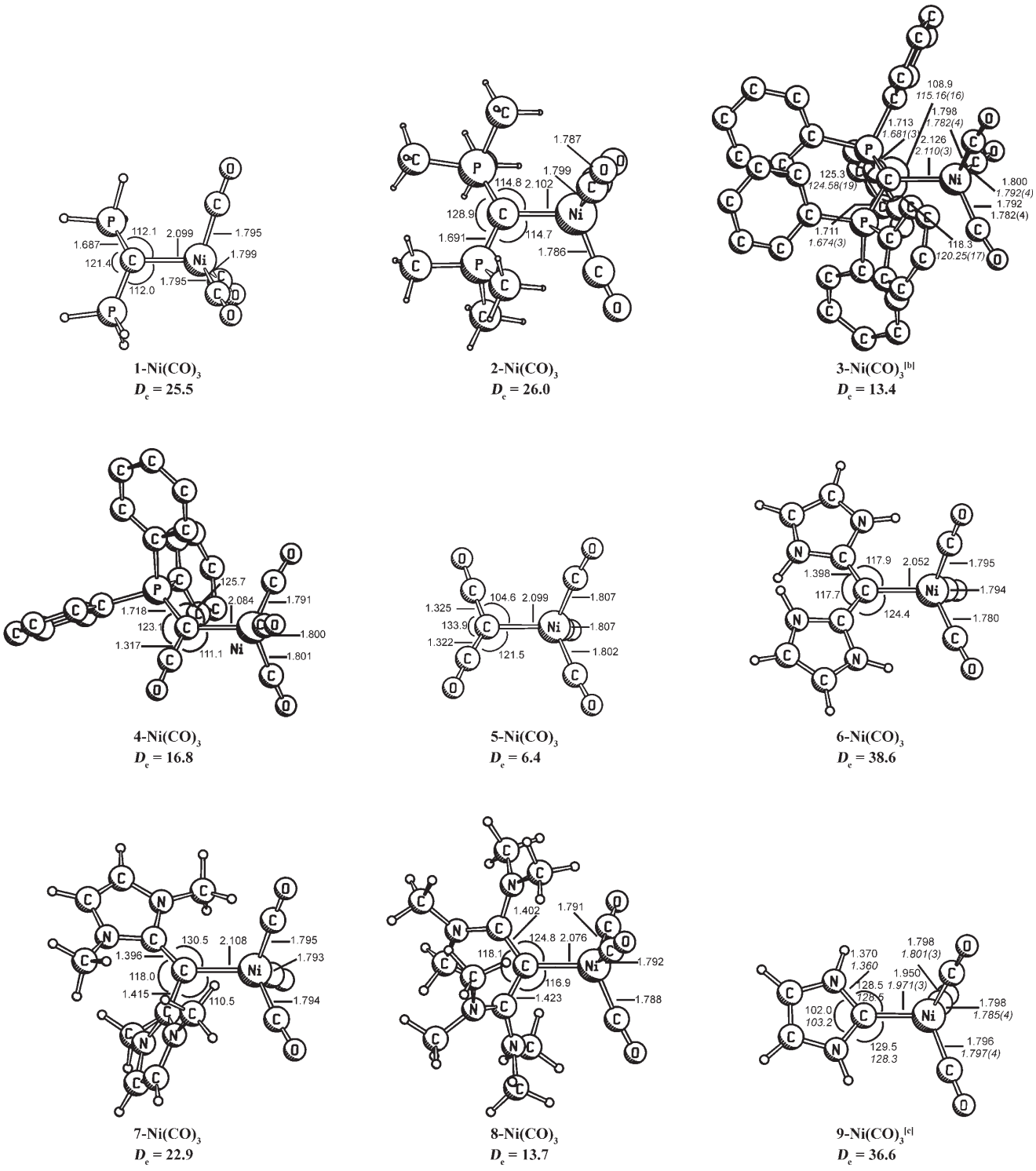

Figure 4. (Continued)

of the CL_2 ligands have positive values except for the C_3O_2 ligand in **5-Ni(CO)$_3$** and **5-Ni(CO)$_2$** and the mixed Ph_3P-C-CO ligand in **4-Ni(CO)$_2$** (Table 7). The negative value of q-(CL_2) may be caused by $L_2C\leftarrow TM$ π backdonation when L = CO. Note that the tungsten atom in the complexes always carries a significant negative charge, while the nickel atom is always positively charged in N–Ni(CO)$_n$. Atomic partial charges are frequently taken as indicators for the electrostatic interaction between bonded atoms. This would mean that the L_2C–TM(CO)$_n$ bond in the tungsten complexes would experience electrostatic repulsion, while the nickel complexes would be stabilized by electrostatic attrac-

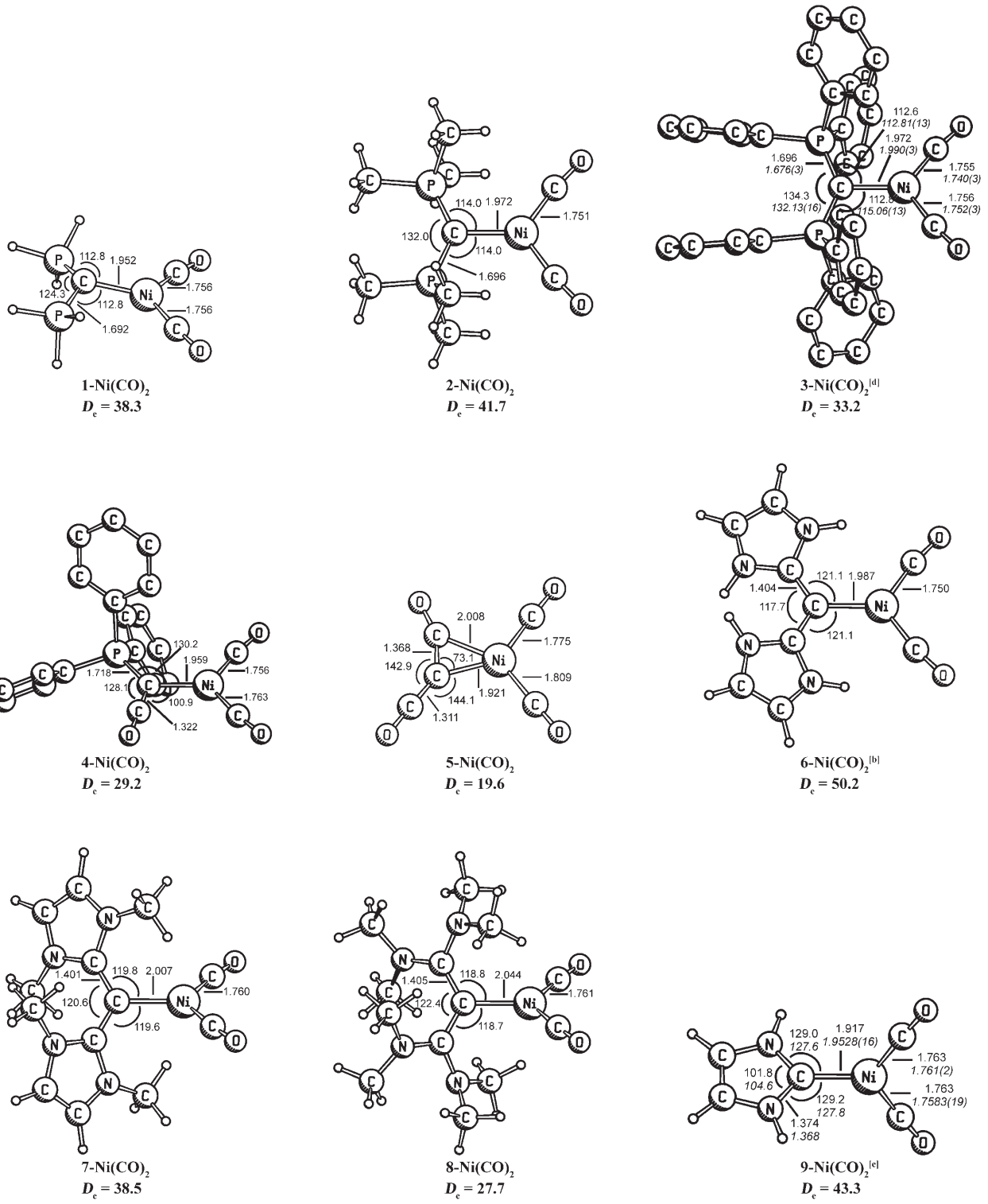

Figure 4. (Continued)

tion. This conclusion is not justified, because atomic partial charges are the sum over the whole atomic basin, which does not give any information about the spatial distribution of the electronic charge. The $L_2C\rightarrow TM$ bond mainly comes from the carbon σ lone pair, which induces strong electrostatic attraction due to overlap with the metal nucleus. This becomes obvious in the calculated electrostatic interactions given by the EDA results, which are presented next.

Table 8 gives the EDA results for the metal complexes **N-W(CO)$_5$**, **N-Ni(CO)$_3$** and **N-Ni(CO)$_2$** for **N**=**1**, **5**, **6**, and **9**.

Table 7. NBO results (BP86/TZVPP//BP86/SVP) for **N-W(CO)$_5$**, **N-Ni(CO)$_3$**, **N-Ni(CO)$_2$** (**N** = **1**–**9**). Atomic partial charges [e] are given for the central carbon atom [q(C)], the metal atom (q(M)) and the whole CL_2 fragment [$q(CL_2)$].

			L^1 L^2C–TM								
			W(CO)$_5$			Ni(CO)$_3$			Ni(CO)$_2$		
	L^1	L^2	q(C)	$q(CL_2)$	q(M)	q(C)	$q(CL_2)$	q(M)	q(C)	$q(CL_2)$	q(M)
1-TM	PH_3	PH_3	−1.34	+0.30	−0.66	−1.41	+0.11	+0.41	−1.47	+0.06	+0.34
2-TM	PMe_3	PMe_3	−1.41	+0.34	−0.60	−1.52	+0.17	+0.44	−1.59	+0.12	+0.37
3-TM	PPh_3	PPh_3	−1.41	+0.27	−0.59	−1.47	+0.08	+0.46	−1.55	+0.03	+0.35
4-TM	PPh_3	CO	−0.95	+0.24	−0.63	−1.04	+0.07	+0.41	−1.09	−0.01	+0.35
5-TM	CO	CO	−0.64	+0.12	−0.64	−0.68	−0.10	+0.31	−0.68	−0.32	+0.39
6-TM	NHC_H	NHC_H	−0.45	+0.41	−0.65	−0.54	+0.22	+0.43	−0.63	+0.18	+0.35
7-TM	NHC_{Me}	NHC_{Me}	−0.53	+0.37	−0.62	−0.59	+0.17	+0.43	−0.64	+0.15	+0.29
8-TM	$C(NMe_2)_2$	$C(NMe_2)_2$	−0.45	+0.38	−0.61	−0.53	+0.19	+0.44	−0.57	+0.13	+0.31
9-TM	HN=CH–CH=NH		+0.19	+0.32	−0.72	0.04	+0.13	+0.41	+0.01	+0.13	+0.27

The data for the other compounds are not shown because they do not significantly contribute to the bonding analysis. We also show the EDA results for the metal–CO bonds of $W(CO)_6$ and $Ni(CO)_4$ for comparison.[53] The calculated energy terms suggest that the **N-W(CO)$_5$** bonds have more pronounced electrostatic than covalent character. The ΔE_{elstat} values are always larger than the ΔE_{orb} term. The orbital interactions in **N-W(CO)$_5$** mainly come from the σ orbitals which contribute 73–75% to the ΔE_{orb} term. The rather small π-bonding contribution distinguishes the latter bonds from the OC–$W(CO)_5$ bond, which has a stronger π-bonding contribution than σ-bonding contribution (Table 8). The nature of the chemical bonding in the nickel complexes **N-Ni(CO)$_3$** is very similar to the tungsten analogues **N-W(CO)$_5$**. The π contribution to the ΔE_{orb} term in the former species is even smaller than in the latter compounds. This is also the main difference between the **N-Ni(CO)$_3$** and the **OC-Ni(CO)$_3$** bonds. The latter has a stronger π-bonding contribution than σ-bonding contribution. Note that the electrostatic attraction in the nickel complexes **N-Ni(CO)$_3$** is very similar to that of the tungsten analogues **N-W(CO)$_5$** although the atomic partial charges at the N–Ni bonds have opposite signs while the N–W bonds have the same sign (Table 8).

It could be assumed that the shorter and stronger N–Ni bonds in the 16-electron complexes **N-Ni(CO)$_2$** have a larger contribution from $L_2C\rightarrow Ni$ π donation from the second lone-pair orbital of the carbon donor atom than in the 18-electron complexes **N-Ni(CO)$_3$**. Comparison of the $\Delta E_{\pi\perp}(b_1)$ values in the former molecules with the data for $\Delta E_{\pi}(a'')$ of the latter species shows indeed a larger contribution of $\pi_\perp$ donation, which amounts to 15.0% of the ΔE_{orb} term in **N-Ni(CO)$_2$**, while $\Delta E_{\pi}(a'')$ donation in **N-Ni(CO)$_3$** contributes only 7.4%. The former value is still significantly smaller than the 26.8% of π bonding calculated for the OC-$Ni(CO)_3$ bond (Table 8). Note that the nickel atom in **N-Ni(CO)$_2$** has a planar configuration which is typical for a 16-electron complex, and therefore the electron demand of the metal atom is less than in the 18-electron complexes **N-Ni(CO)$_3$**. The nature of the $(CO)_2C$–$Ni(CO)_n$ bond significantly changes from $n=3$, for which the carbon suboxide ligand is η^1-bonded, to $n=2$, for which it is η^2-bonded. The latter species has a significantly more covalent bond (ΔE_{orb} = 49.9%) than the former (ΔE_{orb} = 39.1%) which comes mainly from the in-plane (a′) orbital interactions.

It is interesting to compare the electron density in the carbon–metal bonding region of **N-TM** with the AIM method. Figure 5 shows the Laplacian distribution of **1-Ni(CO)$_2$**, **1-Ni(CO)$_3$** and **1-W(CO)$_5$** in two different views. The droplet-shaped area of charge concentration at the carbon donor atom of **1** which points toward the metal atoms ($\nabla^2\rho(r)<0$, solid lines) is more roundly shaped than that of the CO ligand. This holds for both planes, which are shown on the left and right side of Figure 5. The more flattened shape of the charge concentration at the carbon atom of the CO ligand indicates stronger π interaction of the TM–CO bond compared to the TM–**1** bond. There are only subtle differences between the Laplacian distributions in the Ni–**1** bonding region of **1-Ni(CO)$_2$** and **1-Ni(CO)$_3$**. The area of charge concentration in the former has a more elliptical shape than in the latter, which indicates that the stronger **1**→$Ni(CO)_2$ charge donation comes from enhanced σ donation rather than from π donation.

Conclusion

The theoretical results for the protonated species **N-H$^+$** and **N-(H$^+$)$_2$** and for the complexes **N-BH$_3$**, **N-(BH$_3$)$_2$**, **N-CO$_2$**, **N-(CO$_2$)$_2$**, **N-W(CO)$_5$**, **N-Ni(CO)$_3$**, and **N-Ni(CO)$_2$** are evidence for the statement made in our preceding paper[1] that the chemistry of divalent carbon(0) compounds exhibits unusual features. Compounds **1**–**4** and **6**–**9** are very strong electron donors; this becomes manifest in the calculated protonation energies, which reach values of up to 300 kcal mol^{-1} for **7**, and in very high bond strengths of the donor–acceptor complexes. The calculations show that the experimentally known compounds $C(PMe_3)_2$ (**2**), $C(PPh_3)_2$ (**3**), $C(PPh_3)(CO)$ (**4**), $C(CO)_2$ (**5**) and $(Me_2N)_2C{=}C{=}C(NMe_2)_2$ (**8**) react with electron deficient species such as molecules L_2C which have two L→C donor–acceptor bonds and a carbon atom that has two electron lone pairs. This behavior is not directly obvious when the linear structures of carbon suboxide and tetraaminoallenes are considered. It only

Table 8. EDA [kcal mol^{-1}] results (BP86/TZ2P) of **N-W(CO)$_5$**, **N-Ni(CO)$_3$** and **N-Ni(CO)$_2$** where **N** = **1**, **5**, **6**, **9**, CO. The **N-W(CO)$_5$** and **N-Ni(CO)$_2$** complexes (except **5-Ni(CO)$_2$**) were optimized under C_{2v} symmetry constraints; for **N-Ni(CO)$_3$** and **5-Ni(CO)$_2$** C_s symmetry was applied.

			N-W(CO)$_5$		
	1-W(CO)$_5$	**5-W(CO)$_5$**	**6-W(CO)$_5$**	**9-W(CO)$_5$**	**OC-W(CO)$_5$**
ΔE_{int}	−47.0	−20.0	−60.9	−57.8	−49.6
ΔE_{Pauli}	95.4	51.1	128.6	123.3	118.6
ΔE_{elstat}[a]	−95.0 (66.7)	−38.4 (54.0)	−132.7 (70.0)	−128.5 (70.9)	−89.7 (53.3)
ΔE_{orb}[a]	−47.5 (33.3)	−32.7 (46.0)	−56.9 (30.0)	−52.6 (29.1)	−78.6 (46.7)
$\Delta E_{\sigma}(a_1)$[b]	−35.4 (74.6)	−23.8 (72.7)	−42.1 (74.0)	−38.6 (73.3)	−36.3 (46.1)
$\Delta E_{\delta}(a_2)$[b]	−0.6 (1.2)	−0.4 (1.3)	−1.2 (2.1)	−0.5 (0.9)	0.0 (0.0)
$\Delta E_{\pi\perp}(b_1)$[b]	−6.0 (12.7)	−3.0 (9.0)	−7.3 (12.9)	−9.1 (17.3)	−21.2 (26.9)
$\Delta E_{\pi\parallel}(b_2)$[b]	−5.5 (11.6)	−5.6 (17.0)	−6.3 (11.0)	−4.5 (8.5)	−21.2 (26.9)
ΔE_{prep}	3.9	4.0	8.4	2.4	3.9
ΔE_{prep} (N)	2.4	3.1	5.8	0.4	0.4
ΔE_{prep} (TM)	1.5	0.9	2.6	2.0	3.5
ΔE ($=-D_e$)	−43.1	−16.0	−52.5	−55.5	−45.7
d(N–TM) [Å]	2.335	2.411	2.357	2.230	2.060
			N-Ni(CO)$_3$		
	1-Ni(CO)$_3$	**5-Ni(CO)$_3$**	**6-Ni(CO)$_3$**	**9-Ni(CO)$_3$**	**CO-Ni(CO)$_3$**
ΔE_{int}	−35.5	−14.4	−50.1	−47.0	−40.4
ΔE_{Pauli}	95.7	59.3	122.8	129.3	129.0
ΔE_{elstat}[a]	−89.7 (68.4)	−44.7 (60.8)	−120.9 (69.9)	−127.1 (72.1)	−101.7 (60.0)
ΔE_{orb}[a]	−41.5 (31.6)	−28.9 (39.2)	−52.0 (30.1)	−49.2 (27.9)	−67.7 (40.0)
$\Delta E_{\sigma}(a')$[b]	−38.4 (92.6)	−26.8 (92.8)	−48.4 (93.2)	−41.4 (84.1)	−49.6 (73.2)
$\Delta E_{\pi}(a'')$[b]	−3.1 (7.4)	−2.1 (7.2)	−3.6(6.8)	−7.8 (15.9)	−18.1 (26.8)
ΔE_{prep}	8.7	7.6	13.6	8.8	11.1
ΔE_{prep} (N)	1.9	3.2	5.0	0.4	0.2
ΔE_{prep} (TM)	6.8	4.4	8.6	8.4	10.9
$\Delta E(=-D_e)$	−26.8	−6.7	−36.4	−38.1	−29.3
d(N–TM) [Å]	2.068	2.137	2.083	1.954	1.815
			N-Ni(CO)$_2$		
	1-Ni(CO)$_2$	**5-Ni(CO)$_2$**	**6-Ni(CO)$_2$**	**9-Ni(CO)$_2$**	
ΔE_{int}	−43.5	−46.4	−61.8	−50.4	
ΔE_{Pauli}	103.4	130.7	129.7	125.6	
ΔE_{elstat}[a]	−101.8 (69.3)	−88.8 (50.1)	−141.2 (73.7)	−131.9 (74.9)	
ΔE_{orb}[a]	−45.1 (30.7)	−88.4 (49.9)	−50.3 (26.3)	−44.1 (25.1)	
$\Delta E_{\sigma}(a_1)$[b]	−32.0 (70.9)		−34.4 (68.3)	−31.3 (70.9)	
$\Delta E_{\delta}(a_2)$[b]	−0.2 (0.5)		−0.4 (0.8)	0.1 −(0.3)	
$\Delta E_{\pi\perp}(b_1)$[b]	−6.8 (15.0)		−6.9 (13.6)	−8.1 (18.2)	
$\Delta E_{\pi\parallel}(b_2)$[b]	−6.1 (13.6)		−8.7 (17.4)	−4.9 (11.1)	
$\Delta E_{\sigma}(a')$[b]		−78.8 (89.2)			
$\Delta E_{\pi}(a'')$[b]		−9.5 (10.8)			
ΔE_{prep}	6.8	27.1	14.3	5.8	
ΔE_{prep}(N)	1.7	15.9	5.7	0.3	
ΔE_{prep}(TM)	5.1	11.2	8.5	5.5	
ΔE ($=-D_e$)	−36.7	−19.3	−47.5	−44.6	
d(N–TM) [Å]	1.953	1.919	2.001	1.927	

[a] The values in parentheses are the percentage contributions to the total attractive interactions $\Delta E_{elstat}+\Delta E_{orb}$. [b] The values in parentheses are the percentage contributions to the total orbital interactions ΔE_{orb}.

comes to the fore on reaction with strong electron acceptors. The calculations predict that single and double protonation of **5** and **8** take place at the central carbon atom, where the negative charge increases upon subsequent protonation. The hitherto experimentally unknown carbodicarbenes **6** and **7** are predicted to be even stronger Lewis bases than carbodiphosphoranes **1**–**3**.

We hope that the results presented here and in our preceding paper[1] will be helpful as a guideline and that they will stimulate experimental work in the field. We are convinced that the chemistry of divalent carbon(0) is full of surprising discoveries which are waiting for inventive chemists. Finally, we point out that the bonding model of two donor–acceptor bonds L→E←L may also be found for main group atoms other than E = C, and it may not be restricted to a coordination number of two. We are currently exploring the extension of the donor–acceptor model to other species.

Acknowledgements

This work was supported by the Deutsche Forschungsgemeinschaft. Excellent service by the Hochschulrechenzentrum of the Philipps-Universität Marburg is gratefully acknowledged. Further computer time was pro-

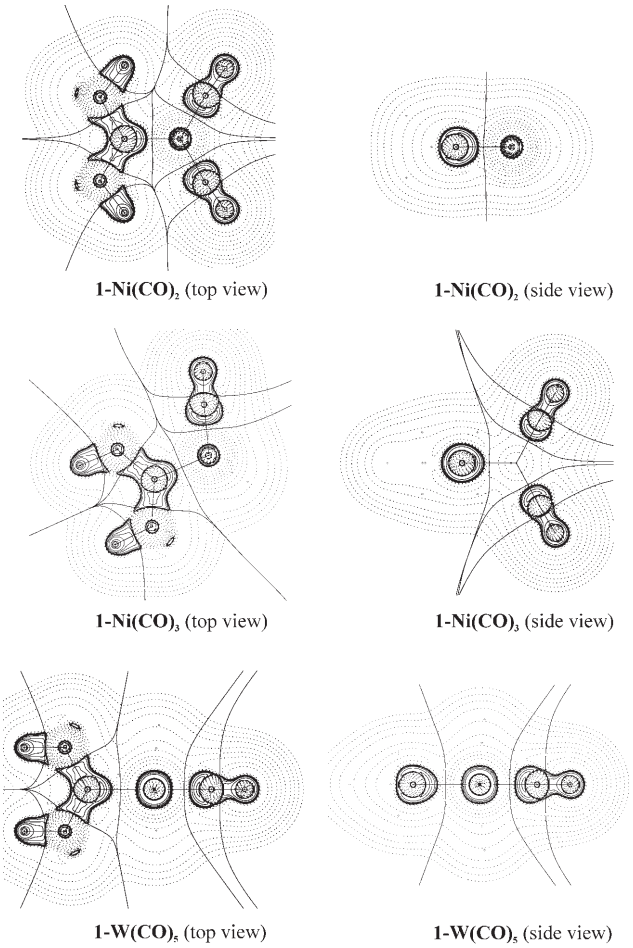

Figure 5. Contour line diagrams $\nabla^2\rho(r)$ of the transition metal complexes **1-Ni(CO)$_2$**, **1-Ni(CO)$_3$**, and **1-W(CO)$_5$** in two different views. Solid lines indicate areas of charge concentration ($\nabla^2\rho(r)<0$) while dashed lines show areas of charge depletion ($\nabla^2\rho(r)>0$). The thick solid lines connecting the atomic nuclei are the bond paths. The thick solid lines separating the atomic basins indicate the zero-flux surfaces crossing the molecular plane.

vided by the HLRS Stuttgart, the CSC Frankfurt and the HHLRZ Darmstadt.

[1] R. Tonner, G. Frenking, *Chem. Eur. J.* **2008**, *14*, DOI: 10.1002/chem.200701390.
[2] A recent compilation of papers which summarizes the research in the field of allene chemistry comes to the conclusion that "…this chemistry has not been developed further during the last three decades": R. Zimmer, H.-U. Reissig in *Modern Allene Chemistry, Vol. 1*, p. 469, (Eds.: N. Krause, A. S. K. Hashmi), Wiley-VCH, Weinheim, **2004**.
[3] H. G. Viehe, Z. Janousek, R. Gompper, D. Lach, *Angew. Chem.* **1973**, *85*, 581; *Angew. Chem. Int. Ed. Engl.* **1973**, *12*, 566.
[4] M. J. Taylor, P. W. J. Surman, G. R. Clark, *J. Chem. Soc. Chem. Commun.*, **1994**, 2517.
[5] a) R. Tonner, F. Öxler, B. Neumüller W. Petz, G. Frenking, *Angew. Chem.* **2006**, *118*, 8206; *Angew. Chem. Int. Ed.* **2006**, *45*, 8038; b) R. Tonner, G. Frenking, *Angew. Chem.* **2007**, *119*, 8850; *Angew. Chem. Int. Ed.* **2007**, *46*, 8695.
[6] a) A. D. Becke, *Phys. Rev. A* **1988**, *38*, 3098; b) J. P. Perdew, *Phys. Rev. B* **1986**, *33*, 8822.
[7] A. Schaefer, H. Horn, R. Ahlrichs, *J. Chem. Phys.* **1992**, *97*, 2571.
[8] S. Grimme, *J. Chem. Phys.* **2003**, *118*, 9095.
[9] Gaussian 03, Revision D.01, M. J. Frisch et al., Gaussian, Inc., Wallingford CT, **2004**. For full reference see Supporting Information.
[10] R. Ahlrichs, M. Baer, M. Haeser, H. Horn, C. Koelmel, *Chem. Phys. Lett.* **1989**, *162*, 165.
[11] D. Andrae, U. Häussermann, M. Dolg, H. Stoll, H. Preuss, *Theor. Chim. Acta* **1990**, *77*, 123.
[12] A. E. Reed, L. A. Curtiss, F. Weinhold, *Chem. Rev.* **1988**, *88*, 899.
[13] R. F. W. Bader, *Atoms in Molecules: A Quantum Theory*, Oxford University Press, Oxford, **1990**.
[14] a) T. Ziegler, A. Rauk, *Inorg. Chem.* **1979**, *18*, 1755; b) T. Ziegler, A. Rauk, *Inorg. Chem.* **1979**, *18*, 1558; c) K. Morokuma, *J. Chem. Phys.* **1971**, *55*, 1236.
[15] a) F. M. Bickelhaupt, E. J. Baerends in *Reviews In Computational Chemistry, Vol. 15*, Wiley, New York, **2000**, p. 1; b) G. Te Velde, F. M. Bickelhaupt, E. J. Baerends, C. Fonseca Guerra, S. J. A. Van Gisbergen, J. G. Snijders, T. Ziegler, *J. Comput. Chem.* **2001**, *22*, 931.
[16] For further details see Methods Section of ref. [1].
[17] a) E. Van Lenthe, E. J. Baerends, J. G. Snijders, *J. Chem. Phys.* **1993**, *99*, 4597; b) E. Van Lenthe, E. J. Baerends, J. G. Snijders, *J. Chem. Phys.* **1994**, *101*, 9783; c) E. Van Lenthe, A. Ehlers, E. J. Baerends, *J. Chem. Phys.* **1999**, *110*, 8943.
[18] a) F. Ramirez, N. B. Desai, B. Hansen, N. McKelvie, *J. Am. Chem. Soc.* **1961**, *83*, 3539; b) G. E. Hardy, J. I. Zink, W. C. Kaska, J. C. Baldwin, *J. Am. Chem. Soc.* **1978**, *100*, 8002.
[19] Recent reviews: a) N. D. Jones, R. G. Cavell, *J. Organomet. Chem.* **2005**, *690*, 5485; b) O. I. Kolodiazhnyi, *Phosphorous Ylides: Chemistry and Application in Organic Synthesis*, Wiley-VCH, Weinheim, **1999**; c) O. I. Kolodiazhnyi, *Tetrahedron* **1996**, *52*, 1855; d) *Ylides and Imines of Phosphorus* (Ed.: A. W. Johnson), Wiley, New York, **1993**.
[20] W. C. Kaska, D. K. Mitchell, R. F. Reichelderfer, *J. Organomet. Chem.* **1973**, *47*, 391.
[21] W. Petz, C. Kutschera, M. Heitbaum, G. Frenking, R. Tonner, B. Neumüller, *Inorg. Chem.* **2005**, *44*, 1263.
[22] J. Vicente, A. R. Singhal, P. G. Jones, *Organometallics* **2002**, *21*, 5887.
[23] W. Petz, F. Weller, J. Uddin, G. Frenking, *Organometallics* **1999**, *18*, 619.
[24] W. Petz, F. Öxler, B. Neumüller, G. Frenking, R. Tonner, unpublished results.
[25] N. Kuhn, G. Henkel, T. Kratz, J. Kreutzberg, R. Boese, A. H. Maulitz, *Chem. Ber.* **1993**, *126*, 204.
[26] N. Kuhn, M. Steimann, G. Weyers, *Z. Naturforsch. B* **1999**, *54*, 427.
[27] W. Petz, C. Kutschera, S. Tschan, F. Weller, B. Neumüller, *Z. Anorg. Allg. Chem.* **2003**, *629*, 1235.
[28] H. C. Freeman, F. Huq, J. M. Rosalky, I. F. Taylor, Jr., *Acta Cryst. Sect. B* **1975**, *31*, 2833.
[29] Y. P. Makovetskii, N. G. Feshchenko, A. N. Chernega, M. Y. Antipin, Y. T. Struchkov, *Zh. Obshch. Khim.* **1991**, *61*, 1075.
[30] J. D. Walker, R. Poli, *Polyhedron* **1989**, *8*, 1293.
[31] N. Kuhn, H. Bohnen, T. Kratz, G. Henkel, *Liebigs Ann. Chem.* **1993**, 1149.
[32] a) E. Oeser, *Chem. Ber.* **1974**, *107*, 627; b) M. J. Taylor, P. W. J. Surman, G. R. Clark, *J. Chem. Soc. Chem. Commun.* **1994**, 2517.
[33] V. Jonas, G. Frenking, M. T. Reetz, *J. Am. Chem. Soc.* **1994**, *116*, 8741.
[34] We calculated the second protonation energy of **8** in which one nitrogen atom is protonated instead of carbon. The calculated value at MP2/TZVPP//BP86/SVP is 11.6 kcal mol^{-1} smaller than the value for the carbon-diprotonated species.
[35] A. Haaland, *Angew. Chem.* **1989**, *101*, 1017; *Angew. Chem. Int. Ed. Engl.* **1989**, *28*, 992.
[36] R. Tonner, G. Frenking, unpublished results.
[37] W. Petz, C. Kutschera, S. Tschan, F. Weller, B. Neumüller, *Z. Anorg. Allg. Chem.* **2003**, *629*, 1235.
[38] N. Kuhn, A. Al-Sheikh, *Coord. Chem. Rev.* **2005**, *249*, 829.
[39] A. Stasch, S. Singh, H. W. Roesky, M. Noltemeyer, H. G. Schmidt, *Eur. J. Inorg. Chem.* **2004**, 4052.

[40] The rather accurate calculation of two different singlet states with a DFT approach is possible because they have different symmetry ($^1\Delta$ and $^1\Sigma^+$).
[41] K. P. Huber, G. Herzberg, *Molecular Spectra and Molecular Structure IV. Constants of Diatomic Molecules*, Van Nostrand-Reinhold, New York, **1979**.
[42] It is often assumed that the electrostatic attraction between charged species is stronger than between neutral moieties. The assumption ignores the spatial distribution of the electronic charge in a molecule, which is not revealed by atomic partial charges. Striking examples where atomic partial charges are misleading for estimating electrostatic interactions have been presented in ref. [53a] and in J. Uddin, G. Frenking, *J. Am. Chem. Soc.* **2001**, *123*, 1683.
[43] A. Krapp, F. M. Bickelhaupt, G. Frenking, *Chem. Eur. J.* **2006**, *12*, 9196.
[44] S. Erhardt, G. Frenking, *Chem. Eur. J.* **2006**, *12*, 4620.
[45] Interestingly, the neutral and charged complexes $H_3B–EC_5H_5$ and $H_2B^+–EC_5H_5$ (E = N–Bi) show a "normal" correlation between B–E bond length and BDE, that is, the charged species have B–E bonds which are stronger and shorter than in the neutral complexes. This comes from the additional effect of *E*–B π bonding in $H_2B^+–EC_5H_5$. For further details see ref. [44].
[46] This has been discussed in detail in ref. [21].
[47] I. Hyla-Kryspin, S. Grimme, *Organometallics* **2004**, *23*, 5581.
[48] N. Kuhn, T. Kratz, R. Boese, D. Bläser, *J. Organomet. Chem.* **1994**, *470*, C8.
[49] R. Dorta, E. D. Stevens, N. M. Scott, C. Costabile, L. Cavallo, C. D. Hoff, S. P. Nolan, *J. Am. Chem. Soc.* **2005**, *127*, 2485.
[50] K. E. Lewis, D. M. Golden, G. P. Smith, *J. Am. Chem. Soc.* **1984**, *106*, 3905.
[51] W. C. Kaska, D. K. Mitchell, R. F. Reichelderfer, *J. Organomet. Chem.* **1973**, *47*, 391.
[52] S. Z. Goldberg, K. N. Raymond, *Inorg. Chem.* **1973**, *12*, 2923.
[53] For recent discussions of the bonding situation in metal carbonyls, see: a) A. Diefenbach, F. M. Bickelhaupt, G. Frenking, G. *J. Am. Chem. Soc.* **2000**, *122*, 6449; b) A. J. Lupinetti, G. Frenking, S. H. Strauss, *Angew. Chem.* **1998**, *110*, 2229; *Angew. Chem. Int. Ed.* **1998**, *37*, 2113; c) A. J. Lupinetti, S. H. Strauss, G. Frenking, *Prog. Inorg. Chem., Vol. 49* (Ed.: K. D. Karlin), Wiley, New York, **2001**, p. 1; d) G. Frenking, N. Fröhlich, *Chem. Rev.* **2000**, *100*, 717.

Received: September 4, 2007
Revised: December 10, 2007
Published online: March 3, 2008

